A Dynamic Strategic Plan for the Transition to a Clean Bus Fleet using Multi-Stage Stochastic Programming with a Case Study in Istanbul

Neman Karimi[a], Burak Kocuk[a,*], Tuğçe Yüksel[a,b]

[a] *Faculty of Engineering and Natural Sciences, Sabancı University, Istanbul, Turkey*
[b] *Smart Mobility and Logistics Lab, Sabancı University, Istanbul, Turkey*

Abstract

In recent years, the transition to clean bus fleets has accelerated. Although this transition might bring environmental and economic benefits, it requires a long-term strategic plan due to the large investment costs involved. This paper proposes a multi-stage stochastic program to optimize strategic plans for the clean bus fleet transition that explicitly considers the uncertainty scenarios in the cost and efficiency improvements of clean buses. Our optimization model minimizes the total expected cost subject to emission targets, budget restrictions and several other operational considerations. We propose a new forecasting approach that captures the correlation between these improvements to obtain realistic future pathways for Battery Electric Buses (BEBs) and Hydrogen Fuel Cell Buses (HFCBs), which are then given to the multi-stage stochastic program as scenarios. We also utilize a physics-based model for BEBs to accurately capture their energy consumption and recharging needs. As a case study, we focus on the complex public bus network of Istanbul, which aims to transition to a clean bus fleet by 2050. Utilizing real datasets, we solve a five-stage stochastic program spanning a 25-year planning horizon that involves 256 scenarios to obtain dynamic strategic plans that can be used by the policy makers. Our results suggest that BEBs are more advantageous than HFCBs, even in slow BEB but fast HFCB development scenarios. We also conduct several sensitivity analyses to understand the effects of the intermediate emission targets, budget limitations and energy prices.

Keywords: `OR in Energy, Bus fleet transition, Zero-emission vehicles, Multi-stage stochastic programming`

1. Introduction

Transport-related CO_2 emissions account for over 21% of global emissions, with the majority coming from internal combustion engine vehicles used in road transport (IEA, 2023b). Due to the significant impact of these emissions on climate change, ambitious targets have been set to transition the transport sector from fossil fuels to sustainable energy sources. For instance, the United States aims to eliminate all emissions

*Corresponding author
Email addresses: `neman.karimi@sabanciuniv.edu` (Neman Karimi), `burak.kocuk@sabanciuniv.edu` (Burak Kocuk), `tugce.yuksel@sabanciuniv.edu` (Tuğçe Yüksel)

in the transport sector by 2050, while the European Union pledges to reduce transport-related emissions by 90% by the same year (European Commission, 2020; Muratori et al., 2023). Although the adoption of clean energy alternatives such as electric and fuel cell vehicles has increased in recent years, a lot more effort is still needed to keep the long-term net-zero emission goals within reach. This is particularly important for medium and heavy-duty vehicles such as trucks and buses, which need accelerated transitions (IEA, 2023a). Despite making up only 8% of all vehicles (excluding two- and three-wheelers), trucks and buses account for over 35% of road transport emissions (IEA, 2024b). To accelerate the shift of these vehicles to clean technology alternatives, 33 countries have joined the Global Memorandum of Understanding on Zero-Emission Medium- and Heavy-Duty Vehicles as of 2023, committing to 30% zero-emission truck and bus sales by 2030 and 100% by 2040 (IEA, 2024a).

Such policies and pledges necessitate strategic planning to minimize the total costs of transitioning heavy-duty vehicle fleets, such as city buses. Due to the currently high investment costs of zero-emission buses—including their purchase and the costs related to building the required infrastructure— carefully constructed strategic plans could save millions of dollars. These plans should focus on identifying the most cost-effective mix of bus technologies to purchase, the most favorable infrastructure technology to utilize (such as overnight charging vs. fast charging for electric buses), and the optimal timing for bus replacements. To this end, case studies have been conducted for several cities worldwide, including cities in China (Zhang et al., 2022), Singapore (Zhou et al., 2023), Germany (Dirks et al., 2022), France (Pelletier et al., 2019), the US (Islam & Lownes, 2019), and Austria (Frieß & Pferschy, 2024), to optimize the bus fleet transition to clean energy buses.

Most of the relevant studies focused on electric buses (EB) as the clean energy option. With today's technology, EBs are widely considered to be the most cost-effective zero-emission alternative. However, their integration into fleets is complicated by a number of barriers, the most significant being their limited driving range. Currently, battery electric buses (BEBs), which rely only on electricity stored in on-board batteries, are the most common type of EBs. There are different options available for BEBs in terms of battery capacity which can affect operational planning during their use. BEBs equipped with large and heavy batteries might be recharged only at night due to the long recharging time, or those that have smaller batteries can utilize fast charging stations and possibly recharge multiple times within the day to ensure demand satisfaction. Assuming that existing bus dispatch timetables are maintained, it is crucial to ensure that buses relying on overnight charging (ONC) have sufficient battery capacity to complete the scheduled trips. Moreover, fast-charging (FC) buses require an additional consideration in recharge scheduling, which depends on the frequency of assigned trips, availability of charging stations and the time needed for recharging. To this end, different studies have attempted to optimize the decisions related to the investment and placement of charger technology, investments on electric buses with different battery capacities and recharge scheduling (Perumal et al., 2022).

Hydrogen fuel cell buses (HFCBs) are also gaining attention in the literature. Although they may not yet be competitive with EBs, efforts to reduce their purchase and operational costs could make them promising

options for new city buses in near future. These buses are similar to diesel buses in terms of their operation, as they usually require one daily refueling, which takes less than 10 minutes (Anandarajah et al., 2013).

Many efforts are being made to improve both BEBs and HFCBs in terms of reducing costs and increasing efficiency. For BEBs, the anticipated increase in energy density of batteries will improve their driving range, allowing them to operate on lines that were previously impractical or not cost-effective. Improvements in HFCBs are also expected to increase fuel cell efficiency, thereby decreasing fuel consumption and lowering operational costs. However, these improvements in cost and efficiency are often overlooked in strategic transition plans for bus fleets. Anticipated cost reductions are only rarely considered as yearly reductions in the purchase cost of BEBs and in a deterministic manner. Efficiency-related improvements and their implications are even more scarce in the literature. In He et al. (2023), reductions in energy consumption of newly purchased buses and increased recharging efficiency were included, but again as deterministic parameters.

To the best of our knowledge, no study has included long-term technological advances in BEBs and HFCBs, which are uncertain by nature, affecting their costs and efficiency as stochastic scenarios. To fill this gap, we present an optimization model to strategically plan the bus fleet transition to clean energy technologies, treating cost- and efficiency-related technological advances in batteries and fuel cells as scenarios in a large-scale multi-stage stochastic programming model. After forecasting the advances and clustering them into scenarios in order to capture their inherent correlation, we test our model on the large bus fleet of Istanbul Municipality, which aims to transition to a clean bus fleet by 2050 as part of its Sustainable Urban Mobility Plan (Istanbul Metropolitan Municipality, 2022), with more than 6,500 buses operating on over 830 lines. We also perform sensitivity analysis to provide insights for bus fleet owners and managers.

1.1. Literature Review

The literature on strategic planning for transitioning to clean energy buses can be categorized into two main approaches: 'one-step transition' and 'multi-step transition.' In the one-step transition approach, strategic decisions, including investments in fleet and infrastructure, are made at a single point in time. In contrast, the multi-step transition approach involves making decisions at multiple points throughout the planning period, usually because of budget constraints or long-term emission reduction goals. This gradual transition approach is better suited for taking into account evolving technologies and changing parameters; therefore, we adopt this approach in the current paper. In what follows, we first mention some one-step transition studies before delving into the literature on multi-step transition.

Existing studies with a one-step transition approach are mostly focused on electric buses and their necessary infrastructure. Different charging technologies, including recharging at stations, lane charging, and battery swap technologies were evaluated against each other in some studies (Bi et al., 2017; Chen et al., 2018). However, the majority of studies focused on charging stations and involved the deployment of fast-charging and overnight depot charging stations in their strategic plans. This includes optimal placement of fast-charging stations (Xylia et al., 2017), decisions about battery capacity (Kunith et al., 2017), and in-

vestigating the effect of factors like demand uncertainties (An, 2020) and energy consumption uncertainty (Benoliel et al., 2021) on such decisions. Some researchers integrated more operational-level problems such as electric bus scheduling and charge scheduling, with strategic decisions including infrastructure planning, battery sizing and fleet sizing, see, e.g., He et al. (2022), Rogge et al. (2018), Shehabeldeen et al. (2024), and Yıldırım and Yıldız (2021).

On the other hand, most studies with a multi-step approach developed optimization models similar to those for the parallel equipment replacement problem. In these models, purchasing and salvaging decisions are made in each period to minimize total costs while ensuring demand is met throughout the planning horizon. Keles and Hartman (2004) were among the first to apply such models to bus fleets, including different competing technologies. Later studies incorporated emission-related costs (Feng & Figliozzi, 2014) or constraints (Emiliano et al., 2020), along with decisions for bus-to-task assignments (Stasko & Gao, 2010). Islam and Lownes (2019) included BEBs as clean technology options and accounted for their charger costs. An integer linear program developed by Pelletier et al. (2019) aimed to minimize total fleet management costs, incorporating various charging technologies for electric buses, midlife costs for BEB batteries, and bus-to-route assignments. Tang et al. (2021) addressed diesel-electric replacement ratios to manage potential fleet size increases due to range anxiety associated with BEBs.

Some recent multi-step transition studies integrated strategic decisions with various operational-level decisions. Dirks et al. (2022) addressed charging station deployment and battery sizing decisions, along with operational decisions such as assigning electric buses to routes and tracking battery state of charge. Zhang et al. (2022) incorporated seasonal variations in electric bus consumption into their model. Zhou et al. (2023) used an aggregated demand approach and considered external costs, including climate and health impacts, battery replacement costs, and evaluated different types of electric and hybrid buses. Li et al. (2022), focused on determining charger locations, planning bus route electrification, and assigning buses to charging stations in a Build-Operate-Transfer setting. He et al. (2023) accounted for future technological advances such as reduced battery and charger costs, and improved charging efficiency in a deterministic setting. This study included siting and sizing of fast-charging stations along with recharge schedules for new BEBs.

In Table 1, we compare various studies on multi-step bus fleet transition and highlighting their key aspects. To the best of our knowledge, no study has incorporated the uncertainty of future ZEB improvements into strategic planning for bus fleet transitions. As both BEBs and HFCBs are still developing, incorporating these uncertainties into planning ensures that strategies remain adaptable and cost-effective as advancements occur. The current absence of HFCBs in many strategic plans is largely due to their higher costs and lower efficiency compared to BEBs, an aspect that should be reconsidered as the future technological improvements could make HFCBs more competitive. Additionally, no study has considered the impact of route-specific energy consumption of BEBs, seasonal variations in their consumption rate, and diesel-electric replacement ratios together in strategic planning. To fill these gaps in the literature, we present a multi-stage stochastic program that incorporates technological developments while also considering detailed operational consider-

ations, providing a comprehensive and adaptive solution for bus fleet transition planning.

Table 1: Studies on multi-step bus fleet transition.

		Decisions			EB Operational Feasibility				Technological Change		
Reference	Bus Technologies	Fleet Invest.	Charger Invest.	Task Assign.	Calculating Electricity Consumption	Recharge Scheduling	Seasonal Effect	Diesel-electric Replacement Ratio	Cost	Efficiency	Stochasticity
Stasko and Gao (2010)	DB	✓	-	✓	-	-	-	-	✗	✗	✗
Feng and Figliozzi (2014)	DB/HEB	✓	-	✗	-	-	-	-	✓	✗	✗
Islam and Lownes (2019)	DB/HEB/BEB	✓	✓	✗	✗	✗	✗	✗	✓	✗	✗
Pelletier et al. (2019)	DB/CNG/BEB	✓	✓	✓	✗	✗	✗	✗	✓	✗	✗
Emiliano et al. (2020)	DB	✓	-	✗	-	-	-	-	✗	✗	✗
Tang et al. (2021)	DB/HEB/BEB	✓	✓	✗	✗	✗	✗	✓	✓	✓	✗
Li et al. (2022)	BEB	✓	✓	✓	✗	✓	✗	-	✓	✗	✗
Dirks et al. (2022)	DB/BEB	✓	✓	✓	✗	✓	✗	-	✓	✗	✗
Zhang et al. (2022)	DB/BEB	✓	✓	✓	✓	✓	✓	-	✓	✗	✗
Zhou et al. (2023)	DB/HEB/BEB	✓	✓	✗	✗	✗	✗	✗	✓	✗	✗
He et al. (2023)	BEB	✓	✓	✓	✓	✓	✗	-	✓	✓	✗
This Paper	DB/BEB/HFCB	✓	✓	✓	✓	✓	✓	✓	✓	✓	✓

DB: Diesel, BEB: Battery Electric, HFCB: Hydrogen Fuel Cell, CNG: Compressed Natural Gas, HEB: Hybrid Electric

1.2. Our Approach and Contributions

In this paper, we develop a multi-stage stochastic program, in which the future costs and efficiencies of competing clean technologies are represented as nodes in a scenario tree. Decisions regarding purchasing and salvaging the buses and assigning them to routes will be made on a yearly basis, and a dynamic transition plan will guide the fleet managers to make optimal decisions in each scenario throughout the planning horizon. We then test our model on a large bus fleet in Istanbul, including BEBs utilizing ONC or FC technology, as well as HFCBs. To account for operational feasibility of replacing diesel buses with electric options, we pre-calculate the energy consumed by each type and version of BEB on a given route. Using a heuristic method, we estimate the diesel-electric replacement ratio for each electric bus, on each route, and under each scenario. We provide an extensive case study involving real data collected from various sources, and conduct sensitivity analyses regarding the underlying stochastic process, the emission targets, budget limitations and energy prices. Our main contributions to the literature are listed as below.

- We introduce a multi-stage stochastic program for the fleet replacement problem, and investigate the effect of uncertain technological advances on the optimal long-term transition plan of vehicle fleets.
- We forecast the technological improvements of both BEBs and HFCBs in terms of cost reductions and efficiency improvements, and cluster them into a number of scenarios.
- We test our model on the large bus network of Istanbul for a 25-year planning horizon with five stages, involving details such as the energy consumption calculation of several versions of BEBs on each bus line, energy consumption changes with seasonal variations, and ensuring operational feasibility by finding the diesel-electric replacement ratios and recharge scheduling for FC electric buses.

We note that although we focus on a bus fleet transition problem in Istanbul, the idea of modeling technology advances as scenarios and incorporating them into a multi-stage stochastic program is applicable to other

energy transition problems, emphasizing both the novelty and the generalization potential of our work.

The rest of this paper is organized as follows: Section 2 provides a detailed explanation of the problem and our methodology. Section 3 describes the data requirements and how we obtain the parameters for our case study. Section 4 presents the case study and sensitivity analysis. Finally, Section 5 concludes the paper.

2. Methodology

This section provides a detailed explanation of our methodological approach. We begin with a conceptual description of the problem in Section 2.1, followed by the mathematical formulation in Section 2.2. Next, in Section 2.3, we explain the method for estimating the amount of energy consumed by the BEBs with different configurations, when assigned to each scheduled trip. Finally, in Section 2.4, we describe our *Bus-to-Route Simulator*, which is run to obtain key parameters of our optimization model if a specific bus is assigned to a route.

2.1. Problem Description

Bus fleet operators face the challenge of determining the optimal long-term transition plan from DBs to zero-emission buses (ZEBs) such as BEBs and HFCBs. The goal is to minimize the total costs of managing the fleet over a planning horizon subject to emission targets, budget limitations and other operational requirements. Let us denote $\mathscr{T} = \{0, 1, \ldots, T\}$ as the time periods in the planning horizon, where decisions on purchasing, salvaging, and assigning buses to routes are made at the beginning of each time period. Time period 0 is used to initiate the existing fleet, and no actual decisions are made in this time period. From time period 1 onwards, bus fleet operators must decide for each bus whether to keep it (if it has not reached its economic lifetime) or to replace it with one of the available bus technologies in the market.

Accounting for the technological advancements of ZEBs is essential for planning a cost-effective transition as these advancements can significantly improve performance and reduce costs. However, the uncertain nature of these advancements makes it challenging to determine the optimal timing for ZEB investments. To tackle this complex task, we introduce a multi-stage stochastic program with S stages, where each stage consists of a collection of time periods. We follow the classical scenario tree based representation (Shapiro et al., 2021) where nodes within each stage represent possible states of all technologies over these periods in terms of cost and efficiency. Although our formulation below works for any given scenario tree $\mathscr{N}$, we specify how we construct it according to our case study in Section 3.4.

Before formally providing our formulation, we list our assumptions below:

- Each time period represents a year, as bus fleet operators typically make decisions based on the yearly budget. We further divide each year into subperiods (seasons) to account for potential differences in route demand and variations in BEB and HFCB consumption rates due to seasonal factors.
- The time periods within each stage share the same stochastic characteristics.

- Different versions may exist for each type of technology, reflecting variations such as the brand and model of the bus. For example, one version of a BEB might be a 12-meter model with a 280 kWh battery capacity, using fast-charging stations, with a 12-year lifespan, and priced at 440,000 USD.
- Investment costs of BEBs include charger cost upon purchase and battery replacements cost at their mid-life. The manufacturer commits to providing battery replacements to account for battery degradation.
- All BEBs, regardless of charging type, start the day with a full battery.
- A ZEB cannot be salvaged before reaching half of its economic lifetime.
- Demand is known in advance and is deterministic.
- Assuming the passenger capacity is the same for all buses of the same length, each bus can be replaced only by another bus of the same length.
- As the cost and energy density of lithium-ion batteries (Li-ion) improve, larger batteries will be installed on BEBs while maintaining the same overall weight, but with a smaller unit cost. This will allow a BEB to cover longer distances.
- As the cost and efficiency of fuel cell systems improve, purchase cost as well as O&M cost of HFCBs will decrease due to the fact that improved efficiency of fuel cell systems will reduce the energy consumption per unit distance.
- Recharging takes a fixed amount of time, depending on the battery capacity of the BEB versions. We assume charging power also advances alongside BEB technological improvements so that the recharging time remains consistent even after the improvement.
- Deadheading (trips with no passengers) between terminals is allowed, and buses consume less energy in such trips. However, deadheading trips to and from garages are disregarded.
- Only tailpipe emissions are considered and the emissions related to electricity and hydrogen production are not included.

2.2. Mathematical Formulation

In this section, we present the mathematical formulation of our multi-stage stochastic program for transitioning to a clean bus fleet. The model aims to optimize decisions regarding the purchasing, salvaging, and assigning of buses to routes while considering technological advancements over a planning horizon. We present the index sets, decision variables and parameters used in our mathematical formulation in Tables 2, 3 and 4, respectively.

Table 2: List of index sets.

Set	Description	Set	Description
$\mathcal{N}$	Set of nodes, $\mathcal{N} = \{0,1,\ldots,N\}$	$\mathcal{T}$	Set of time periods, $\mathcal{T} = \{0,1,\ldots,T\}$
$\mathcal{N}_f$	Set of nodes in the final stage	$\mathcal{T}_n$	Set of time periods containing node n
$\mathcal{J}$	Set of bus types	$\mathcal{T}_{(t']}$	Set of time periods t s.t. $t \leq t'$ and $t + \omega_{(j,t)} > t'$
$\mathcal{K}_j$	Set of versions for bus type j	$\mathcal{T}_{[t')}$	Set of time periods t s.t. $t < t'$ and $t + \omega_{(j,t)} \geq t'$
$\mathcal{R}$	Set of routes	$\mathcal{T}_{(t')}$	Set of time periods t s.t. $t < t'$ and $t + \omega_{(j,t)} > t'$
$\mathcal{Q}$	Set of subperiods of each time period	$\mathcal{T}^-_{[t')}$	Set of time periods t s.t. $t + \lceil \omega_{(j,k,t)}/2 \rceil \leq t'$ and $t + \omega_{(j,k,t)} \geq t'$

Table 3: List of decision variables.

Variable	Description
$v^{+}_{(j,k,t),n}$	Number of version $k \in \mathscr{K}_j$ of bus type $j \in \mathscr{J}$ purchased in time period $t \in \mathscr{T}_n$ and node $n \in \mathscr{N}$.
$v_{(j,k,t),t',n}$	Number of version $k \in \mathscr{K}_j$ of bus type $j \in \mathscr{J}$ purchased in time period $t \in \mathscr{T}$ and available in time period $t' \in \mathscr{T}_n$ and node $n \in \mathscr{N}$, subject to $t \leq t' < t + \omega_{(j,k,t)}$.
$v'_{(j,k,t),t',r,q,n}$	Number of version $k \in \mathscr{K}_j$ of bus type $j \in \mathscr{J}$ purchased in time period $t \in \mathscr{T}$ and assigned to route $r \in \mathscr{R}$ in subperiod $q \in \mathscr{Q}$ of time period $t' \in \mathscr{T}_n$ and node $n \in \mathscr{N}$, subject to $t \leq t' < t + \omega_{(j,k,t)}$.
$v^{-}_{(j,k,t),t',n}$	Number of version $k \in \mathscr{K}_j$ of bus type $j \in \mathscr{J}$ purchased in time period $t \in \mathscr{T}$ and salvaged in time period $t' \in \mathscr{T}_n$ and node $n \in \mathscr{N}$, subject to $t + \lceil \omega_{(j,k,t)}/2 \rceil \leq t' \leq t + \omega_{(j,k,t)}$.

Table 4: List of parameters.

Parameter	Description
π_n	Probability of node $n \in \mathscr{N}$
$\mu_{(n,t)}$	The node corresponding to the ancestor of node $n \in \mathscr{N}$ at time $t \in \mathscr{T}$
$\beta_{nominal}$	Nominal discount rate applied to time periods
ζ	Inflation rate applied to time periods
β_{real}	Real discount rate, calculated as $\beta_{real} = \frac{1+\beta_{nominal}}{1+\zeta} - 1$
β	Discount factor, calculated as $\beta = \frac{1}{1+\beta_{real}}$
$\delta^{+}_{(j,k,t),n}$	Investment cost of version $k \in \mathscr{K}_j$ of bus type $j \in \mathscr{J}$ purchased in time period $t \in \mathscr{T}_n$ at node $n \in \mathscr{N}$
$\delta^{-}_{(j,k,t),t',n}$	Salvage value of version $k \in \mathscr{K}_j$ of bus type $j \in \mathscr{J}$ purchased in time period $t \in \mathscr{T}$ and salvaged in time period $t' \in \mathscr{T}_n$ at node $n \in \mathscr{N}$
$\delta_{(j,k,t),t',r,q,n}$	Operational and maintenance costs of version $k \in \mathscr{K}_j$ of bus type $j \in \mathscr{J}$ purchased in time period $t \in \mathscr{T}$, operated in time period $t' \in \mathscr{T}_n$, assigned to route $r \in \mathscr{R}$ in subperiod $q \in \mathscr{Q}$, and at node $n \in \mathscr{N}$
$\omega_{(j,k,t)}$	Economic life of version $k \in \mathscr{K}_j$ of bus type $j \in \mathscr{J}$ purchased in time period $t \in \mathscr{T}_n$
$\lambda_{(j,k,t),t',r,q,n}$	Demand satisfaction ratio of version $k \in \mathscr{K}_j$ of bus type $j \in \mathscr{J}$ purchased in time period $t \in \mathscr{T}$, operated in time period $t' \in \mathscr{T}_n$, assigned to route $r \in \mathscr{R}$ in subperiod $q \in \mathscr{Q}$, and at node $n \in \mathscr{N}$
$\Delta_{t,r,q}$	Demand in subperiod $q \in \mathscr{Q}$ of route $r \in \mathscr{R}$ at time period $t \in \mathscr{T}$
γ_t	Available budget for time period $t \in \mathscr{T}$
$\varepsilon_{(j,k,t),t'}$	Emissions of version $k \in \mathscr{K}_j$ of bus type $j \in \mathscr{J}$ purchased in time period $t \in \mathscr{T}$ and operated in time period $t' \in \mathscr{T}$
η_t	Maximum allowable emissions for time period $t \in \mathscr{T}$
$\phi_{j,k}$	Initial fleet size of version $k \in \mathscr{K}_j$ of bus type $j \in \mathscr{J}$
ψ	Maximum desired average age of the fleet at the end of the planning horizon

We now present our multi-stage stochastic program as below:

$$\min \sum_{n=1}^{N} \pi_n \sum_{j \in \mathscr{J}} \sum_{k \in \mathscr{K}_j} \left(\sum_{t \in \mathscr{T}_n} \beta^{(t-1)} \delta^{+}_{(j,k,t),n} v^{+}_{(j,k,t),n} + \sum_{t' \in \mathscr{T}_n} \sum_{t \in \mathscr{T}_{(t']}} \sum_{r \in \mathscr{R}} \sum_{q \in \mathscr{Q}} \beta^{(t'-1)} \delta_{(j,k,t),t',r,q,n} v'_{(j,k,t),t',r,q,n} \right.$$

$$\left. - \sum_{t' \in \mathscr{T}_n} \sum_{t \in \mathscr{T}_{[t')}} \beta^{(t'-1)} \delta^{-}_{(j,k,t),t',n} v^{-}_{(j,k,t),t',n} \right) \tag{1a}$$

$$\text{s.t.} \sum_{j\in\mathscr{J}}\sum_{k\in\mathscr{K}_j}\sum_{t\in\mathscr{T}_{(t')}} \lambda_{(j,k,t),t',r,q,n}\, v'_{(j,k,t),t',r,q,n} \geq \Delta_{t',r,q}, \quad t'\in\mathscr{T}_n, r\in\mathscr{R}, q\in\mathscr{Q}, n\in\mathscr{N} \tag{1b}$$

$$\sum_{r\in\mathscr{R}} v'_{(j,k,t),t',r,q,n} \leq v_{(j,k,t),t',n}, \quad j\in\mathscr{J}, k\in\mathscr{K}_j, q\in\mathscr{Q}, t'\in\mathscr{T}_n, t\in\mathscr{T}_{(t')}, n\in\mathscr{N} \tag{1c}$$

$$v_{(j,k,t),t,n} = v^{+}_{(j,k,t),n}, \quad j\in\mathscr{J}, k\in\mathscr{K}_j, t\in\mathscr{T}_n, n\in\mathscr{N} \tag{1d}$$

$$v_{(j,k,t),t',n} = v_{(j,k,t),t'-1,\mu_{(n,t'-1)}} - v^{-}_{(j,k,t),t',n}, \quad n\neq 0, j\in\mathscr{J}, k\in\mathscr{K}_j, t'\in\mathscr{T}_n, t\in\mathscr{T}_{(t')}, n\in\mathscr{N} \tag{1e}$$

$$v^{-}_{(j,k,t),t',n} = v_{(j,k,t),t'-1,\mu_{(n,t'-1)}}, \quad n\neq 0, j\in\mathscr{J}, k\in\mathscr{K}_j, t'\in\mathscr{T}_n, t\in\mathscr{T}_{(t')}, t' = t+\omega_{(j,k,t)}, n\in\mathscr{N} \tag{1f}$$

$$\sum_{j\in\mathscr{J}}\sum_{k\in\mathscr{K}_j} \delta^{+}_{(j,k,t),n}\, v^{+}_{(j,k,t),n} \leq \gamma_t, \quad t\in\mathscr{T}_n, n\in\mathscr{N} \tag{1g}$$

$$\sum_{j\in\mathscr{J}}\sum_{k\in\mathscr{K}_j}\sum_{t\in\mathscr{T}_{(t')}}\sum_{r\in\mathscr{R}}\sum_{q\in\mathscr{Q}} \varepsilon_{(j,k,t),t'}\, v'_{(j,k,t),t',r,q,n} \leq \eta_{t'}, \quad t'\in\mathscr{T}_n, n\in\mathscr{N} \tag{1h}$$

$$v^{+}_{(j,k,0),0} = \phi_{j,k},\ v^{-}_{(j,k,0),0,0} = 0, \quad j\in\mathscr{J}, k\in\mathscr{K}_j \tag{1i}$$

$$\sum_{j\in\mathscr{J}}\sum_{k\in\mathscr{K}_j}\sum_{t\in\mathscr{T}_{(T]}} (T-t+1)\, v_{(j,k,t),T,n} \leq \psi \sum_{j\in\mathscr{J}}\sum_{k\in\mathscr{K}_j}\sum_{t\in\mathscr{T}_{(T]}} v_{(j,k,t),T,n}, \quad n\in\mathscr{N}_f \tag{1j}$$

$$v^{+}_{(j,k,t),n} \in \mathbb{Z}_+, \quad j\in\mathscr{J}, k\in\mathscr{K}_j, t\in\mathscr{T}_n, n\in\mathscr{N} \tag{1k}$$

$$v^{-}_{(j,k,t),t',n} \in \mathbb{Z}_+, \quad j\in\mathscr{J}, k\in\mathscr{K}_j, t'\in\mathscr{T}_n, t\in\mathscr{T}_{[T)}, n\in\mathscr{N} \tag{1l}$$

$$v_{(j,k,t),t',n} \in \mathbb{Z}_+,\ v'_{(j,k,t),t',n} \in \mathbb{Z}_+, \quad j\in\mathscr{J}, k\in\mathscr{K}_j, t'\in\mathscr{T}_n, t\in\mathscr{T}_{(T]}, n\in\mathscr{N}. \tag{1m}$$

The terms in the objective function (1a) represent the investment costs of the buses, the operational and maintenance costs, and the salvage revenue, respectively. Constraints (1b) require that the number of buses assigned to a route in each time period and node meets the required demand. Constraints (1c) specify that the number of assigned buses should not exceed the number of buses available. Constraints (1d) and (1e) maintain the balance of buses for each type and version in every time period. Constraints (1f) ensure that the buses will be salvaged once they reach their economic lifetime. Constraints (1g) restrict the total purchasing costs to stay within the allocated budget for each time period, and constraints (1h) ensure that emissions remain within the limits for each time period. Constraints (1i) define the initial fleet size for each type and version of the bus, and make sure that no buses are salvaged at stage 0. To mitigate end-of-horizon effects, constraints (1j) limit the average age of the buses at the end of the planning horizon. Finally, constraints (1k), (1l), and (1m) ensure that decision variables take non-negative integer values.

2.3. Energy Requirement Calculation

In order to ensure operational feasibility of assigning buses to routes, and optimizing the assignment decisions, it is crucial to account for the amount of energy consumed by each version of BEBs on scheduled trips of different routes. We now present our physics-based approach to calculate the energy requirement of a specific BEB assigned to a given service trip, which impacts the O&M costs and the demand satisfaction ratio parameters. Table 5 provides the notations used in this section.

Table 5: List of parameters for traction power and battery power calculations.

Parameter	Description	Parameter	Description
f_r	Rolling resistance coefficient	ρ_{air}	Air density (kg/m^3)
C_D	Drag coefficient	g	Gravitational acceleration (m/s^2)
A_f	Frontal area of the bus (m^2)	η_t	Transmission efficiency
η_m	Motor and inverter efficiency	η_{rb}	Regenerative braking efficiency
m	Mass of the bus (kg)	m_{eq}	Equivalent mass (kg)
α	Road grade (rad)	$a(\tau)$	Bus acceleration rate at time τ (m/s^2)
$v(\tau)$	Speed of the bus at time τ (m/s)	$P_w(\tau)$	Traction power at time τ (W)

To calculate the energy requirement for a bus on a specific service trip, we first divide the trip into a set $\mathscr{S}$ of segments, where each segment represents the path between two consecutive bus stops. We assume that the bus will accelerate between the time interval $[0, \tau_1]$ with a constant rate of $a > 0$, maintain a constant speed between $[\tau_1, \tau_2]$, and decelerate with rate $-a$ between $[\tau_2, \tau_1 + \tau_2]$. For each segment, we minimize the duration $\tau_1 + \tau_2$ to cover its distance subject to the constraints on maximum speed and maximum power, where the *traction power* $P_w(\tau)$ at time τ is calculated as

$$P_w(\tau) = \left(mg\sin(\alpha) + f_r mg\cos(\alpha) + 0.5\rho_{\text{air}} C_D A_f v(\tau)^2 + m_{\text{eq}} a(\tau)\right) v(\tau).$$

Here, traction power $P_w(\tau)$ refers to the power required at the wheels to overcome resistance forces acting on the bus when traveling at a speed of $v(\tau)$, and accelerate an equivalent mass of m_{eq}, which accounts for the inertial resistance of the rotating masses in the vehicle, with an acceleration of $a(\tau)$. Required traction power is provided by the battery at a higher rate due to losses at the electric motor and transmission elements before reaching the wheels. In addition, during braking or travelling downhill, BEBs can recuperate some of the power that otherwise would be lost as heat via their regenerative braking system. The power required from the battery during traction (or recuperated by the battery during regenerative braking) $P_{\text{bat}}(\tau)$ is given by

$$P_{\text{bat}}(\tau) = \begin{cases} \frac{P_w(\tau)}{\eta_t \eta_m}, & \text{if } P_w(\tau) \geq 0 \\ P_w(\tau) \cdot \eta_t \cdot \eta_m \cdot \eta_{\text{rb}}, & \text{if } P_w(\tau) < 0 \end{cases}.$$

To find the energy requirement E_{s} of segment s, we integrate $P_{\text{bat}}(\tau)$ over the segment duration as $E_{\text{s}} = \int_0^{\tau_1+\tau_2} P_{\text{bat}}(\tau)\, d\tau$. Finally, the total energy required during the trip is the sum of the energy requirements for all segments, computed as $E_{\text{trip}} = \sum_{s\in\mathscr{S}} E_{\text{s}}$. We also account for the variation in energy requirements due to seasonal changes by multiplying the nominal consumption value by a constant that depends on the ambient temperature. We provide the details of power and energy calculations in the Supplementary Material.

2.4. Bus-to-Route Simulator

We develop a simple simulator, Algorithm 1, to estimate key parameters if a version k of bus type j is assigned to a certain route r in a subperiod q. Since the outcome of such an assignment changes over the planning horizon due to technological advances, we run this algorithm for every node n in the scenario tree in an offline manner before solving our optimization model.

Inputs of the Bus-to-Route Simulator are the the specifications of a bus (such as the type, version, charging scheme in case of BEBs, energy consumption, etc.) and the characteristics of the route (such as the trip schedule, road profile, etc.). The simulator aims to minimize the necessary number of buses in a heuristic manner for each assignment while considering operational feasibility of each bus type.

The algorithm outputs the number of necessary buses and their daily task assignments, using which we obtain several parameters used in our optimization model: i) Demand satisfaction ratio $\lambda_{(j,k,t),t',r,q,n}$, defined as the number of buses needed of a specific type-version pair divided by the number of DBs needed. ii) Charger-to-bus ratio for fast-charging BEBs, used in the calculation of the investment cost $\delta^{+}_{(j,k,t),n}$. iii) Average daily distance covered, used in the calculation of the O&M cost $\delta_{(j,k,t),t',r,q,n}$.

3. Data Collection and Processing

In this section, we present the data used in our case study in Section 4. We start by discussing the bus network data provided by the public bus fleet operator of Istanbul in Section 3.1, including a description of the preprocessing steps. Section 3.2 details the initial bus-specific cost information included in our case study. In Section 3.3, we provide the data required for forecasting future technological advancements in BEBs and HFCBs, along with an explanation of our forecasting approach. Finally, in Section 3.4, we explain how the scenarios of our stochastic program are obtained using the resulting projections. We note that the Supplementary Material contains more detailed datasets, analyses and results.

3.1. Public Bus Transit in Istanbul

The buses operated by the Istanbul Electricity, Tram and Tunnel Establishments (IETT), the authority responsible for public bus transportation in Istanbul, carry nearly 5 million people daily and cover approximately 1.2 million kilometers (IETT, 2023). IETT provided us the following datasets:

1. Trip Schedule: This dataset includes the details of service trips scheduled for both March 15, 2023 (Winter Schedule) and August 3, 2023 (Summer Schedule). The summer schedule is assumed to be used only for 92 days during the summer, while the winter schedule is utilized for the remainder of the year. The specific information provided in this dataset is the route code, trip ID, scheduled route start times, scheduled distance, vehicle depot (when available) and vehicle length group.
2. Stop Sequence with Coordinates: This dataset provides the sequence of stops for each route and route type, along with their latitudes and longitudes. Furthermore, we use the Open-Elevation API

Algorithm 1: Bus-to-Route Simulator.

Input: Bus parameters, trip schedule, trip information, terminal-terminal trip information
Output: Bus assignments, recharge details for fast-charging (FC) BEBs, deadheading details

```
for each trip in the scheduled trips do
    if no buses are yet assigned then
        Assign the first bus to the first trip. Move on to the next trip.
    else
        for each assigned bus do
            if the bus's garage location and length match with that of the scheduled trip and the bus
              can reach the trip's start point on time after completing its previous trip, considering
              deadheading then
                if bus is electric then
                    if battery is insufficient for the trip then
                        if bus type is ONC then
                            Skip this bus due to insufficient battery.
                        else if bus type is FC then
                            if the bus can start the trip with the recharge time added then
                                if bus has enough energy to get to the starting point of the trip then
                                    Plan a recharge at the starting point of the trip.
                                else
                                    Plan a recharge where the bus finishes its previous assigned trip.
                                Record recharge details (location, start and end times). Assign the
                                  trip to the bus. Update cumulative energy consumed. Reset battery
                                  capacity. Move on to the next trip.
                            else
                                Skip this bus due to insufficient time for recharging.
                    Assign the trip to this bus. if bus is electric then
                        Update cumulative energy consumed. Update remaining battery capacity.
                    Move on to the next trip.
                else
                    Skip this bus.
    if no current buses can be assigned then
        Assign a new bus to this trip.
for each bus do
    Calculate the assigned distances and energy consumed (if bus is electric), including
      deadheading. if the total assigned distance is less than 10 km then
        Disregard that bus.
Record recharge summary for all fast-charging electric buses and all locations.
```

(Open-Elevation API, 2020) to determine the elevation of each stop.

3. Vehicle Information: This dataset includes information on 3,351 buses operated by IETT, detailing the number of buses at each depot, along with their brand, model, and manufacturing year. It does not cover 3,076 buses under a private bus brand of IETT, for which the detailed data is not available.

We process the above datasets to obtain the following pieces of information.

1. Estimation of Missing Distances: As we do not have the full information about the specific routing of each vehicle, we estimate some distances related to the deadheading services using the Haversine approximation when needed in Algorithm 1 in addition to the distance between consecutive stops.
2. Estimation of Travel Time: Through our preliminary study and dataset received from IETT, we determine that the average speed of buses is approximately 25 km/h. Consequently, we assume a maximum speed of 30 km/h.
3. Calculating Bus Demand: We run our simulator, Algorithm 1, to estimate the number of buses needed of each version to meet the scheduled trips in each route, for both summer and winter schedules. We present the summary of results in Table 6 for DBs. As the total number of buses owned by IETT in 2023 is reported to be 6,652 (IETT, 2023) the algorithm provides a reliable estimation of the actual demand.

Table 6: Total DB demand by length for winter and summer schedules.

Bus Length (m)	**6.5-8**	**8-9**	**10-11**	**11-14**	**14-19**	**Total**
Winter/Summer Schedule	280/269	26/23	12/15	4540/4349	1695/1418	**6553/6071**

4. Route Aggregation: As a preprocessing step, we aggregate routes based on a metric related to the demand satisfaction ratio (DSR). For each route, we calculate the minimum DSR for each BEB version across all bus lengths and seasons using today's technology. These minimum DSRs are then averaged across all BEB versions to create a single metric for each route. Routes are then grouped into 12 clusters based on this metric as follows: $\{\{1.00\}, [0.95, 1.00), [0.90, 0.95), \ldots, [0.50, 0.55), [0.38, 0.50)\}$. As an example, cluster with the metric of 1.00 represents the routes where even the BEB with the smallest battery capacity can cover the scheduled trips in all seasons and all bus length groups used. Since only 13 routes have a metric smaller than 0.50, we group them together into one cluster.

3.2. Initial Bus-Specific Costs

We consider four bus models across different length groups: an 8m model for the 6.5-8m group, a 10m model for both the 8-9 and 10-11m groups, a 12m model for the 11-14m group, and an 18m model for the 14-19m group. Bus purchase costs are estimated from recent tenders in Turkey and Europe, information gathered from local bus manufacturers and technical reports, and given in Table 7. The investment costs of BEBs include battery replacement and charger costs, in addition to the bus purchase costs. We assume that each BEB requires one battery replacement at the end of year six of its operation that is adjusted for the

discount rate. The initial battery pack cost, denoted by BC, is assumed to be 500USD/kWh. For charging infrastructure, our study includes regular chargers with 50kW charging power, priced at 20,000 USD per unit for ONC buses, and fast chargers with 350kW charging power, priced at 45,000 USD per unit for fast charging buses. Each ONC bus requires one dedicated charger while charger-to-bus ratio for FC buses with a specific version is estimated using Algorithm 1 and the total charger cost is distributed across all buses. Recharging times for FC buses are based on a full recharge, assuming a 90% charging efficiency. Finally, we assume that salvage values depreciate yearly by 15% for all buses.

Table 7: Purchase costs (USD) for DBs, BEBs, and HFCBs.

Model	**DB**	**BEB Fast Charging**					**BEB Overnight Charging**					**HFCB**
Length		**140** kWh	**210** kWh	**280** kWh	**350** kWh	**420** kWh	**280** kWh	**350** kWh	**420** kWh	**490** kWh	**560** kWh	
8m	135,000	305,000	340,000	-	-	-	375,000	410,000	-	-	-	500,000
10m	170,000	340,000	375,000	410,000	-	-	410,000	445,000	480,000	-	-	600,000
12m	200,000	370,000	405,000	440,000	475,000	-	440,000	475,000	510,000	545,000	-	700,000
18m	300,000	470,000	505,000	540,000	575,000	610,000	540,000	575,000	610,000	645,000	680,000	1,000,000

The O&M costs include energy, maintenance, and driver costs. We use Algorithm 1 to determine the average daily distance the buses of a specific version cover when assigned a specific route. This information along with the average energy requirement for BEBs is used to calculate the total energy costs and maintenance costs, where the unit costs are given in Table 8. We assume that the energy consumption estimation is done in spring/fall, and increase BEB and HFCB consumption rates by 15% for winter and 5% for summer, consistent with Istanbul's climate. Regarding the driver cost, the information gathered from IETT Activity Reports and Financial Statements suggest that the approximate salary is nearly double the minimum wage. Additionally, the number of drivers is about 20% more than the number of buses. Therefore we assume the driver cost per bus to be 2.4 times the minimum wage, approximately 40 USD/day.

Table 8: Maintenance costs, energy consumption and energy costs for all bus types.

Bus Type	**Energy Consumption**	**Maintenance Cost (USD/**km**)**	**Energy Cost (USD per unit)**
DB	0.435 L/km (Ma et al., 2021)	0.58 (Holland et al., 2021)	1.29 USD/L (Petrol Ofisi, 2024)
BEB	Varies with route and version	0.34 (Holland et al., 2021)	0.16 USD/kWh (Encazip, 2024)
HFCB	0.09 kg/km (Ajanovic et al., 2021)	0.29 (Collins & Post, 2022)	10.00 USD/kg

3.3. Technological Change Forecasts

In this section, we examine the cost and efficiency trends of BEBs and HFCBs. We quantify these trends for each year with respect to five years prior, consistent with our case study (Section 4). Specifically, for each year, the efficiency improvement rate is calculated as the natural logarithm of the year's value divided by the value from five years earlier, while cost improvement is calculated as the negative logarithm of the same ratio. We then plot the scatter plot of these improvement rates, which highlights distinct patterns and trends across five-year periods. Clustering techniques are applied to group the data points based on

their similarities, with each cluster representing a possible scenario of technological advancement. The probabilities associated with each cluster indicate the proportion of data points that belong to that cluster.

3.3.1. BEB Technological Change

The cost of Li-ion batteries per kilowatt-hour has significantly decreased over the years while their energy density has steadily increased. Figure 1a presents the data on energy density and battery cost from 1991 onwards, extracted from the charts in reference Walter et al. (2023) using the WebPlotDigitizer tool (Autometris, 2023). Given the cost and energy density values, we compute the five-year improvement ratios as described above. Then, these ratios are clustered into two and three different groups by minimizing the sum of squared Euclidean distances between each data point and its assigned cluster centers can be seen in Figures 1b and 1c. As an example, let us consider the two-cluster setting, in which case the probabilities for the fast improvement cluster (**F**) and the slow improvement cluster (**S**) are 0.46 and 0.54, respectively. In fast improvement cluster, the energy density and cost improvement rates are 0.27 and 1.05, respectively. Taking the exponential of these rates, we get an energy density multiplier of 1.31 and a cost multiplier of 0.35.

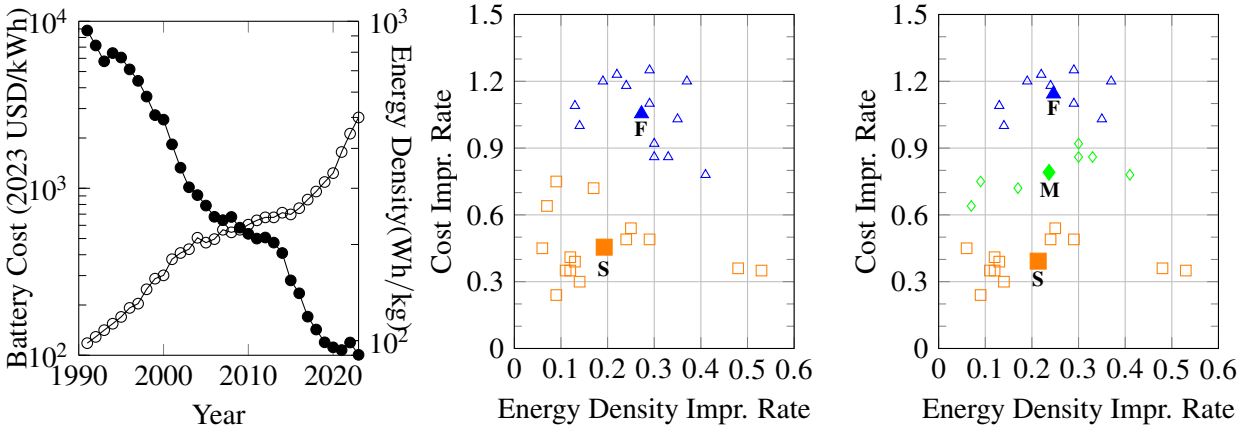

(a) Cell cost (left, solid circle) vs. energy density (right, hollow circle) in log-scale.

(b) Five-year energy density vs. cost improvement rates for BEBs with two clusters.

(c) Five-year energy density vs. cost improvement rates for BEBs with three clusters.

Figure 1: BEB technology improvement charts. Cluster centers are marked with solid marks in (b) and (c), and can be distinguished by the abbreviations of **S**low, **F**ast and **M**edium.

3.3.2. HFCB Technological Change

Fuel cell systems used in HFCBs have also improved in terms of cost and efficiency. However, since these systems are only being used for heavy duty purposes recently, the data is scarce. Instead, we use the cost figures for light duty fuel cell systems (Huya-Kouadio & James, 2023) and the efficiency of a specific producer (Ballard) as a proxy as shown in Figure 2a. We then follow a similar approach to Li-ion batteries: We compute five-year cost and efficiency improvements (for the common years in two datasets), and obtain the clusters in Figures 2b and 2c.

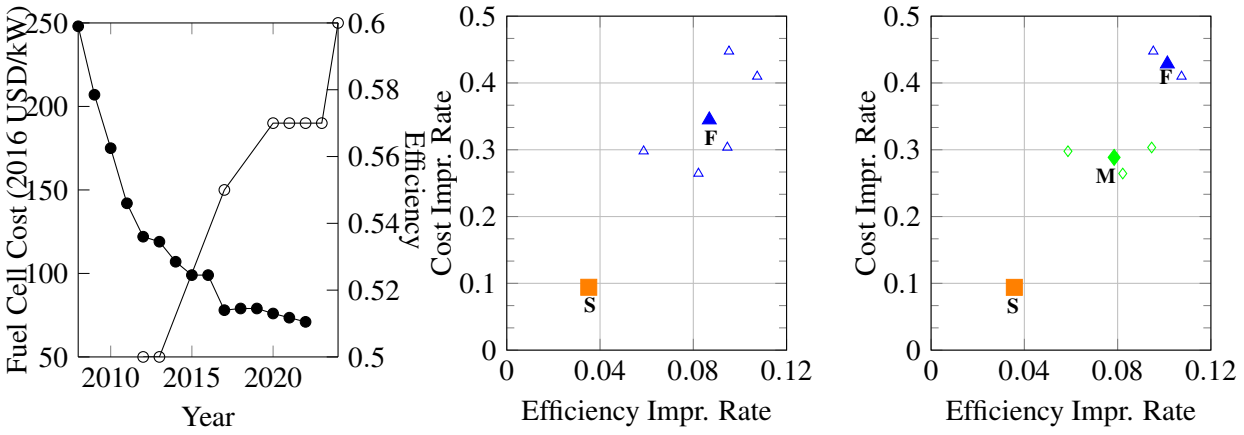

(a) Fuel cell system cost (left, solid circle) vs. efficiency (right, hollow circle).

(b) Five-year efficiency vs. cost improvement rates for HFCBs with two clusters.

(c) Five-year efficiency vs. cost improvement rates for HFCBs with three clusters.

Figure 2: HFCB technology improvement charts.

3.4. Scenario Tree Generation

We now formalize how we obtain the scenarios of our multi-stage stochastic program using the technological change forecasts. Our approach is built on a two-step procedure: In the first step, we obtain *technology trees* for each bus type illustrating future projections while in the second step, we combine these individual projections to build the scenario tree.

Algorithm 2: Technology Tree Construction Algorithm

Input: Improvement distribution of technology j, the number of stages S.

Output: Technology tree.

Set $\theta^c_{j1} = \theta^e_{j1} = \theta^p_{j1} = 1$, ID $= 1$ and $\mathscr{L} = \{1\}$.
for $s = 1, \ldots, S-1$ **do**
  Set $\mathscr{L}' = \emptyset$.
  for $\ell \in \mathscr{L}$ **do**
    for $b = 1, \ldots, B_j$ **do**
      Set ID $=$ ID $+ 1$, $h =$ ID.
      Set $\theta^c_{jh} = \theta^c_{j\ell}\Theta^c_{jb}$, $\theta^e_{jh} = \theta^e_{j\ell}\Theta^e_{jb}$, $\theta^p_{jh} = \theta^p_{j\ell}\Theta^p_{jb}$.
      Set $\mathscr{L}' = \mathscr{L}' \cup \{\text{ID}\}$.
  $\mathscr{L} = \mathscr{L}'$.

Let us start with the first step. For a bus technology $j \in \mathscr{J}$, let us denote its cost and efficiency improvement multipliers for each stage by random variables Θ^c_j and Θ^e_j, respectively, which are assumed to be independent from each other. We will assume that each pair of random variables take values from a joint dis-

crete probability distribution with a sample space consisting of elements $(\Theta^c_{jb}, \Theta^e_{jb})$ w.p. Θ^p_{jb}, $b = 1, \ldots, B_j$. In particular, for a technology j with a given support size B_j, we use the clustering approach from Section 3.3 with B_j clusters, and use efficiency and cost multipliers of each cluster b as $(\Theta^c_{jb}, \Theta^e_{jb})$ values and the fraction of points in each cluster b as Θ^p_{jb}. We run Algorithm 2 to construct a perfect B_j-ary tree denoted by $\mathscr{N}(j)$, which we will call as the technology tree. Figure 3 illustrates exemplary technology trees for DBs, BEBs and HFCBs for $S = 2$ stages with respect to the data reported in Section 3.3.

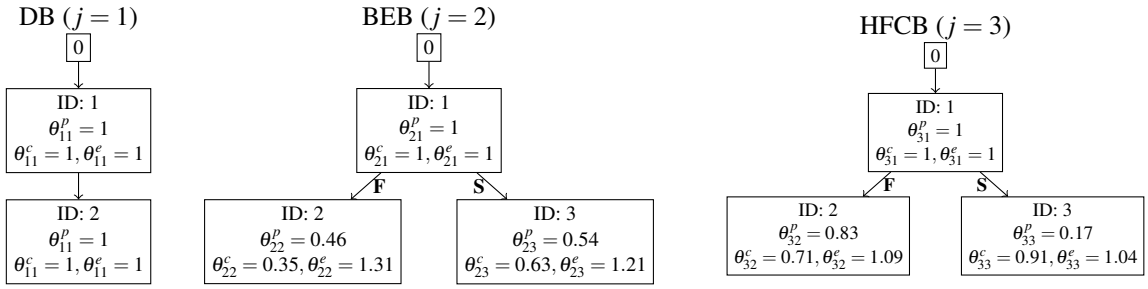

Figure 3: Technology trees of DB ($B_1 = 1$), BEB ($B_2 = 2$) and HFCB ($B_3 = 2$) with $S = 2$ stages.

In the second step, once the technology trees are at hand for each $j \in \mathscr{J}$, we obtain the scenario tree $\mathscr{N}$ by taking the Cartesian product of each node of the technology tree $\mathscr{N}(j)$ at the same level. We label the nodes in the scenario tree in lexicographic order with respect to the node IDs in the technology tree to establish the bijection $n \in \mathscr{N} \leftrightarrow (n_1, n_2, \ldots, n_{|\mathscr{J}|}) \in \mathscr{N}(1) \times \mathscr{N}(2) \times \cdots \mathscr{N}(|\mathscr{J}|)$. This construction can be best explained with an example: Let us consider the scenario tree in Figure 4, which is obtained from the technology trees in Figure 3. The labels of nodes 2, 3, 4, 5 in the scenario tree corresponds to the node ID triplets (2,2,2), (2,2,3), (2,3,2), (2,3,3) in the technology trees.

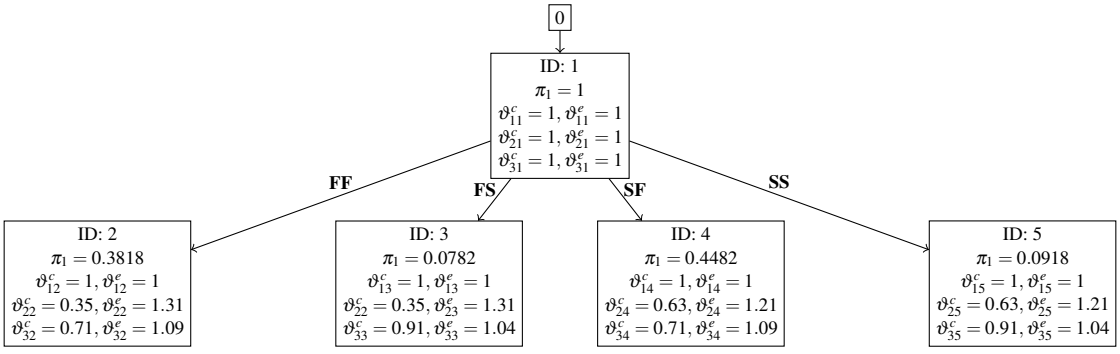

Figure 4: Scenario tree with two stages.

Finally, for each $n \in \mathscr{N}$ and $j \in \mathscr{J}$, we set $\pi_n = \prod_{j \in \mathscr{J}} \theta^p_{j,n_j}$ and $(\vartheta^c_{jn}, \vartheta^e_{jn}) = (\theta^c_{j,n_j}, \theta^e_{j,n_j})$. We note that in a general situation with $|\mathscr{J}|$ many technologies with respective branches of B_j over S stages, the scenario tree will contain $(\prod_{j=1}^{J} B_j)^{S-1}$ leaf nodes (or scenarios), which grows exponentially.

We are now ready to explain how the uncertain parameters are affected in each scenario. We use the abbreviation IC for investment cost, which does not change for DBs over the planning horizon.

For BEBs, technological advances affect the battery capacity (as we assume that the total bus weight remains unchanged) and investment cost. For a specific version with initial battery capacity of C_1, the battery capacity in node n becomes $C_n = C_1 \times \vartheta^e_{BEB,n}$. Then, we run Algorithm 1 to determine the new DSR with battery capacity C_n. Regarding the IC of a BEB of length L in node n with battery capacity C_n, we use

$$\mathrm{IC}_{\mathrm{BEB},n}(L,C_n) = \mathrm{IC}_{\mathrm{DB},1}(L) + \mathrm{CC} + (1+\beta^{\omega/2})[\mathrm{PC} + \mathrm{BC} \times C_n]\vartheta^c_{\mathrm{BEB},n}. \tag{2}$$

Here, PC refers to the cost of other components of the electrified powertrain except the battery and CC stands for the charger cost.

For HFCBs, technological advances affect the investment and O&M costs. In particular, the IC of a HFCB of length L in node n is computed as $\mathrm{IC}_{\mathrm{HFCB},n}(L) = \mathrm{IC}_{\mathrm{DB},1}(L) + [\mathrm{IC}_{\mathrm{HFCB},1}(L) - \mathrm{IC}_{\mathrm{DB},1}(L)]\vartheta^c_{\mathrm{HFCB},n}$ and its consumption rate per distance (CR), which affects the unit energy cost, becomes $\mathrm{CR}_{\mathrm{HFCB},n} = \mathrm{CR}_{\mathrm{HFCB},1}/\vartheta^e_{\mathrm{HFCB},n}$.

4. Case Study

This section presents our case study that focuses on the clean fleet transition in Istanbul public bus network. After we provide our computational setup in Section 4.1, we present the detailed results about our base case in Section 4.2. Then, we provide a thorough sensitivity analyses regarding some key parameters in our case study in Section 4.3. Finally, we compare our stochastic programming model with other approaches in Section 4.4.

4.1. Computational Setup

We conduct our computational experiments in the Python programming language using a 64-bit workstation with two Intel(R) Xeon(R) Gold 6248R CPU (3.00GHz) processors (256 GB RAM). Due to the large-scale nature of the multi-stage stochastic program (1), we relax the integrality restrictions and solve it as a linear program (LP) utilizing Gurobi 11. Since we cluster the routes into categories with a reasonably large demand, continuous variables provide an accurate approximation that can be rounded to obtain practical solutions. In fact, in all cases considered, the difference between the optimal value of the LP relaxation, denoted by z_{LP} and the objective function value of the rounded solution, denoted by z_{round}, is at most 0.23%.

4.2. Base Case

In the `Base Case`, we obtain a dynamic strategic plan of Istanbul's transition to a clean fleet, spanning a planning horizon of 25 years (2025-2049) divided into five stages. We utilize the input data described in Section 3, and set the investment budget in million USD as $\gamma_t = \min\{50t, 250\}$ for $t = 1,\ldots,25$. We also include yearly emission targets, reducing the yearly emission gradually to zero up to year 2049 at a linear rate starting from year 2035. We set the inflation rate $\zeta = 0.04$ and the nominal discount rate as $\beta_{nominal} = 0.05$.

The initial fleet consists of 2,072 7-year-old, 2,817 11-year-old, 318 14-year-old, 635 16-year-old, and 711 18-year-old DBs. The maximum lifetime for buses with an initial age of 11 years or less is assumed to be 16 years, while buses that are 14 years or older are assumed to have a maximum lifetime of 20 years. The remaining lifetime of the initial buses is adjusted accordingly based on these assumptions. Since the fleet is quite old, we assume zero salvage value the existing buses. For newly purchased buses, the economic lifetime is set at 12 years for BEBs and HFCBs, and 15 years for diesel buses. The maximum average fleet age at the end of the planning horizon is capped at 9 years.

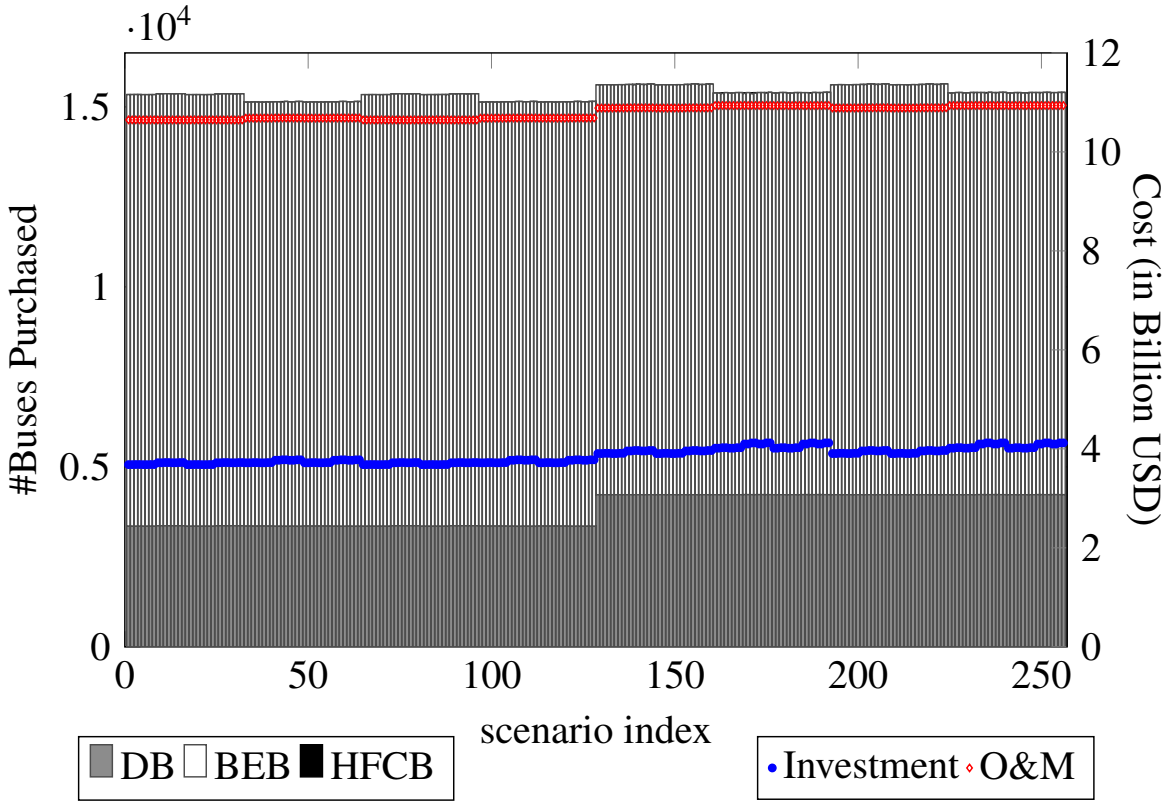

Figure 5: `Base Case` results. Buses purchased are reported with bars and the cost figures are reported with markers.

We consider three technology alternatives: DBs, BEBs and HFCBs. We assume that the cost of DBs do not change, but the cost and efficiency of BEBs and HFCBs improve as explained in Section 3.3 with respect to two clusters each. Therefore, we consider $(1 \times 2 \times 2)^{5-1} = 256$ scenarios in our multi-stage stochastic program. The resulting model contains more than 23 million variables and 3 million constraints. The CPU time is 5,435 seconds, and the expected objective values are $z_{\text{LP}} = 14.126$B USD and $z_{\text{round}} = 14.154$B USD, indicating only a 0.2% difference. For each scenario, we report the number of buses purchased of each technology type along with the total purchase and O&M costs over the planning horizon in Figure 5. Results indicate that the O&M costs are more than twice of the investments costs, which is expected for public buses heavily utilized in Istanbul. In addition, BEBs dominate across all scenarios, while HFCBs are

purchased in small numbers and only in a few scenarios.

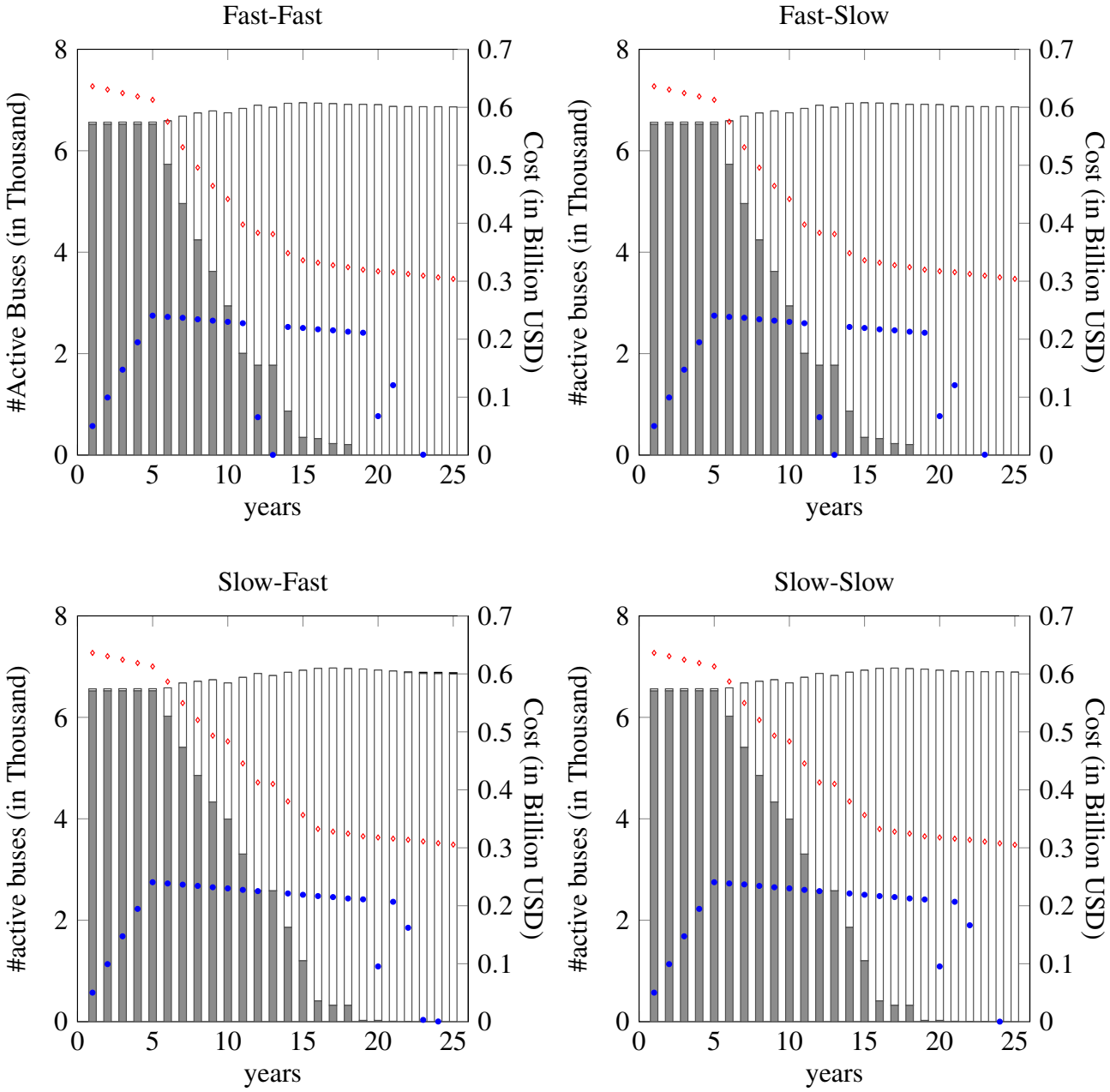

Figure 6: `Base Case`-four specific scenarios.

We also provide detailed results for four particular scenarios in Figure 6: i) Fast-Fast, ii) Fast-Slow, iii) Slow-Fast, iv) Slow-Slow. Here, Fast-Slow refers to the scenario where BEBs improves fast while HFCBs improve slow in each stage (the other three scenarios are defined accordingly). These four scenarios provide

extreme cases and help us illustrate the effect of stochasticity in the dynamic strategic plans. As the initial fleet is quite old, most of the buses need to be retired within the first six years and the budget limitation is most influential in this time frame for all scenarios. We recall that heavily-utilized city buses typically have higher O&M cost in their economic lifetime compared to the initial investment cost. The purchase of BEBs, even in the first year (albeit in small quantities due to budget limitations), shows their advantage over DBs in saving O&M costs. This is especially true for routes where electrification can happen without needing many more buses, that is, routes with DSR values close to 1. We also observe that the fleet size peaks in year 15 for the Fast-Fast and Fast-Slow scenarios, and in year 17 for the Slow-Fast and Slow-Slow scenarios. In the following years, the fleet size slightly decreases due to the higher battery capacities of BEBs purchased in the final stage. The transition to ZEBs is almost complete by year 18 even under the Slow-Slow scenario. Therefore, the zero-emission target can be easily achieved and the adoption to BEBs is also economically justified due to their low O&M costs compared to DBs and HFCBs. Note that HFCBs are only purchased in the last few time periods of the planning horizon, and only in scenarios where the HFCB technology improves fast and BEB technology improves slowly. Even in the most favorable scenario for HFCBs, less than 0.4% of the fleet will be HFCBs in the end.

In Figure 7, We present the bus fleet composition for the first year of Stage 2 through Stage 5, corresponding to years 6, 11, 16, and 21, across two extreme scenarios: Fast-Fast and Slow-Fast. (The results of Fast-Slow and Slow-Slow are omitted, as they are almost identical to those of Fast-Fast and Slow-Fast, respectively.) This figure shows the number of buses of each technology assigned to each cluster during the winter of those years. Recall that Cluster 1 has a DSR value of 1, meaning that it can be electrified with the same number of DBs, while larger cluster labels indicate smaller DSR values, which correspond to routes that may require additional BEBs compared to DBs. The results show that in all scenarios, the transition to BEBs does not begin for clusters 5 through 12 within the first 6 years of the planning period due to their lower DSR values. Additionally, the last four clusters are still using diesel buses during the first 11 years. Cluster 4 is electrified more in the first 6 years than the previous three clusters, likely due to greater savings in O&M costs and the higher age of the initial fleet corresponding to these clusters, among other factors.

We also observe that the few HFCBs purchased in the Slow-Fast scenario are bought in years 22-24 and are almost entirely assigned to cluster 12 to reduce the fleet size in that cluster.

4.3. Sensitivity Analysis

We now present the results of our extensive sensitivity analyses, in which we change some key deterministic parameters of the multi-stage stochastic program that are exogenously determined such as the budget restrictions, emission targets and hydrogen prices. The choice of these parameters are also motivated by our findings from the `Base Case`: i) Budget restrictions are influencing the initial investment decisions, and forcing the model to choose DBs over BEBs due to the lower investment cost of the former despite the lower lifetime cost of the latter. ii) Emission targets are mostly redundant, which enables the model to make the best economical decisions that happen to address the environmental concerns as well. iii) HFCBs are

quite expensive in terms of their O&M costs even without the consideration of potential infrastructure costs, which results in BEBs being the prominent choice for the transition.

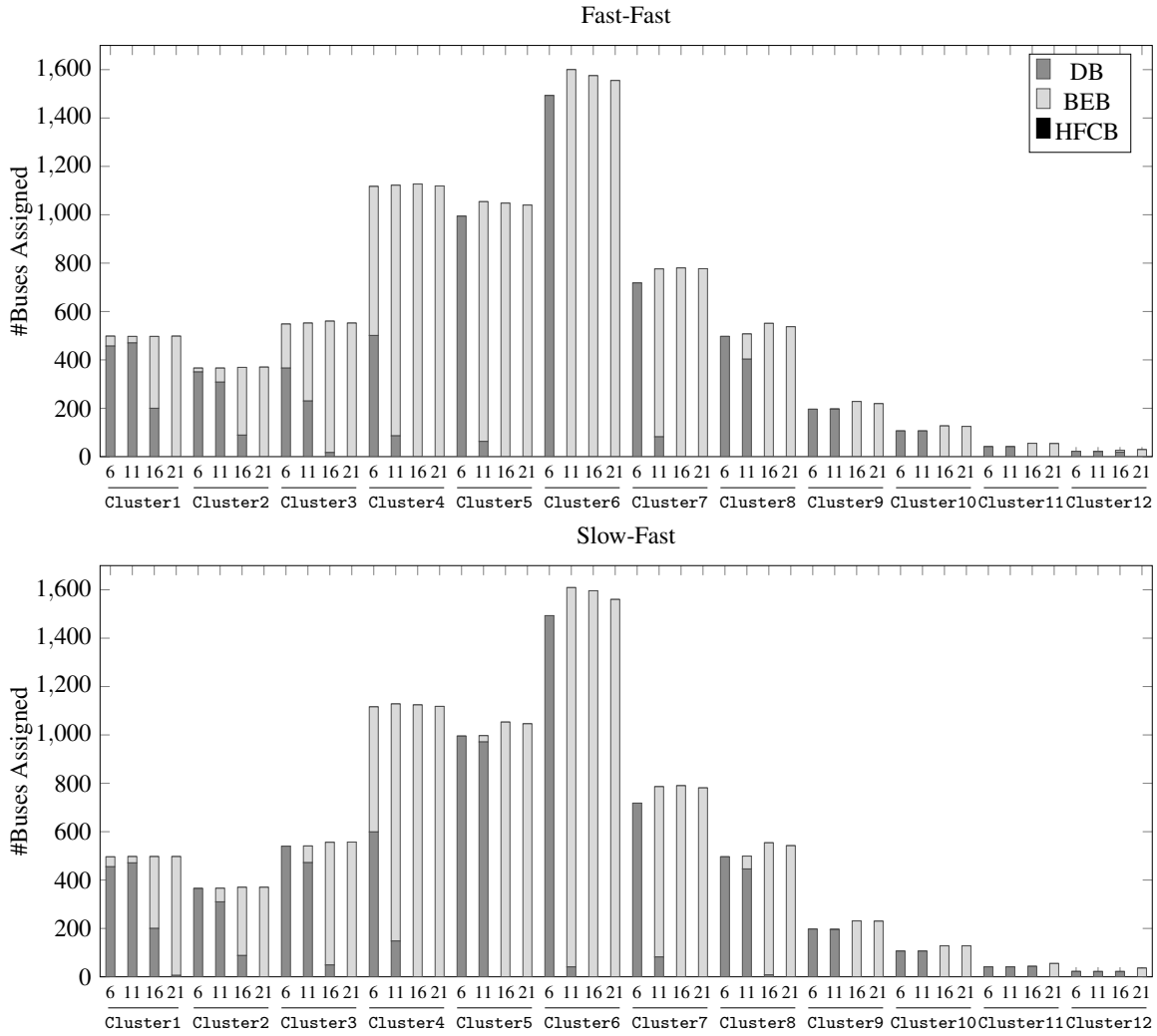

Figure 7: Fleet composition in years 6, 11, 16, 21 under different scenarios with respect to route clusters.

These observations motivate us to explore the answers of the following questions: i) If IETT can spare more budget annually, how much cost benefit can be expected overall? ii) If even more strict emission targets are enforced, how much cost increase can be expected overall? ii) If hydrogen prices drop drastically, can HFCBs become the prominent ZEB choice and how much cost decrease can be expected overall?

To answer these questions, we re-run our multi-stage stochastic model three times for the following cases by keeping everything else the same:

i) `Relaxed Budget`: Budget is chosen 300 Million USD annually.

ii) `Strict Emissions`: Zero emission target is enforced in year 2040 with intermediate targets starting from year 2030.

iii) `Low Hydrogen Price`: Hydrogen price is set at 2 USD/kg.

In Table 9, we provide a summary of the sensitivity analysis conducted while the detailed results are available in the Supplementary Material. We observe that "%Gap", defined as $100 \times \frac{z_{\text{round}} - z_{\text{LP}}}{z_{\text{round}}}$, is consistently small, which suggests that our rounding scheme is quite successful in the new cases as well. In addition, we also report "%Change", which is the percentage change of a new case with respect to the `Base Case` in terms of the objective function value of the rounded solution. As expected, in the `Relaxed Budget Case`, the change is negative, which indicates that an increased budget helps to obtain a more economical plan with 3.80% lower expected cost. Interestingly, the change in the `Strict Emission Case` is very small, which suggests that an even earlier transition to ZEBs can be achieved with increasing the overall cost marginally by 0.08%. Finally, the change in the expected total cost for the `Low Hydrogen Price Case` is also small (-0.17%), which shows the limited effect the hydrogen price has on the overall outcome.

Table 9: Summary results for different cases.

Case	Time (sec)	z_{LP}	z_{round}	%Gap	%Change
`Base`	5,435	14,126,110,527	14,154,103,467	0.20	-
`Relaxed Budget`	5,888	13,586,698,671	13,615,884,770	0.21	-3.80
`Strict Emission`	4,877	14,133,211,491	14,165,320,511	0.23	0.08
`Low Hydrogen Price`	6,133	14,099,073,373	14,129,697,437	0.22	-0.17

We also report the changes in the fleet decomposition and cost figures for the new cases with respect to the `Base Case` under four specific scenarios in Figure 8.

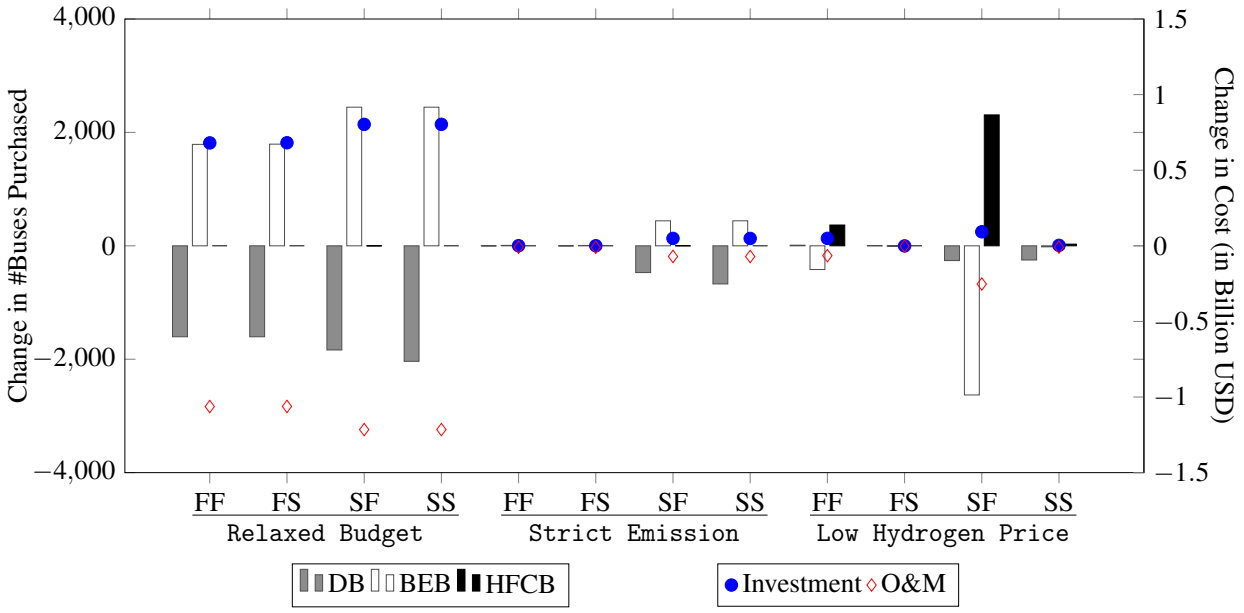

Figure 8: Changes in bus purchases (shown with bars) and cost values (shown with markers) compared to the `Base Case` for four specific scenarios in different cases. FF, FS, SF, SS are respectively the abbreviations of Fast-Fast, Fast-Slow, Slow-Fast, Slow-Slow scenarios as described earlier.

In the `Relaxed Budget Case`, we observe an increase in the number of BEBs purchased across all scenarios as BEBs are economically more advantageous than DBs in their economic lifetime despite their higher investment cost. This is clear from the moderate increase in the investment cost and the substantial decrease in the O&M cost, which is even more pronounced in the Slow-Fast and Slow-Slow scenarios.

In the `Strict Emission Case`, slightly more BEBs are being purchased, with the difference only being non-negligible in scenarios when BEBs improve slowly. This is due to the need to purchase BEBs between 2030 and 2040 to meet emission constraints, even in scenarios where improvements are slow. The small changes with this respect to the `Base Case` illustrate that BEBs are not only environmentally benefical but also cost effective.

In the `Low Hydrogen Price Case`, results indicate that the number of HFCBs purchased increases in most scenarios. In particular, for the four specific scenarios, HFCB purchases increase in three of them, but remain at zero in the Fast-Slow scenario. We also observe that HFCB purchases begin in year 6 in the Slow-Fast scenario, where HFCBs are expected to make up 24.4% of the fleet by the final time period. Nevertheless, as the expected total cost reduction is very small overall, this case suggests that HFCBs will not be dominantly more preferable over BEBs, even if we ignore potential infrastructure costs and potential difficulties regarding hydrogen supply chain.

4.4. Model Comparison

4.4.1. Comparison with a Deterministic Model

To analyze the effect of stochasticity, we solve a deterministic version of our problem and compare its solution with that of the multi-stage stochastic program. In the deterministic model, the technology improvements described in Section 3.3 are represented as a single scenario, reflecting the average of all historical advancements. Specifically, the anticipated cost multipliers for BEBs and HFCBs are 0.48 and 0.74, respectively while the efficiency multipliers are 1.26 and 1.08, respectively. The model solves in 6.4 seconds, and the objective function values are obtained as $z_{\text{LP}} = 13.233$B USD and $z_{\text{round}} = 13.256$B USD. We observe that the deterministic problem's z_{round} value is 0.91B USD (6.43%) lower than that of the stochastic program. This indicates that the solution of deterministic problem cannot be feasible for the stochastic program and we quantify these infeasibilities as described below.

First, we apply the solution of the deterministic problem to each scenario of the stochastic program. To do this, we adjust the battery capacities of BEBs in each scenario based on the capacities from the deterministic solution. However, since energy density improvements vary across scenarios, we need to adjust the bus weights accordingly to reflect the expected improvements in each stochastic scenario. Then, using equation 2, we calculate the BEB investment costs, where C_n (the battery capacity in node n) comes from the deterministic solution, and $\vartheta^c_{\text{BEB},n}$ (the efficiency improvement) relates to each specific scenario. We observe that the deterministic solution violates the budget constraints in 160 out of 256 scenarios of the stochastic program in at least one time period by more than 1%. Considering the probabilities of these scenarios, this means that there is a 67.41% probability that the deterministic solution will not be feasible

due to insufficient budget. Note that these budget violations are even underestimated because, in scenarios where energy density improves more slowly than in the deterministic case, heavier batteries are required, necessitating more buses to meet demand.

Table 10 details the budget violations of the deterministic solution in the stochastic program. Since no HFCBs are purchased in the deterministic problem, it suffices to consider a reduced scenario tree with $2^{5-1} = 16$ scenarios, in which only BEB improvements are considered. In particular, scenarios in Table 10 represent BEB improvements from stage 2 to stage 5 (e.g., FSSF refers to fast improvement in stage 2, slow in stages 3 and 4, and fast again in stage 5). The table shows the percentage of budget violations under different scenarios, and for each year within the stage. For example, the numbers 6.11, 6.76, 6.17, 4.87, 5.15 correspond to the percentage budget violations in years 6, 7, 8, 9, 10 respectively, and under the eight specified BEB improvement scenarios. The observed infeasibilities highlight the importance of stochastic modelling and dynamic planning in strategic decision making. By accounting for uncertainty in technology improvements, the stochastic model avoids the infeasibilities that arise when applying the deterministic solution, ensuring a more robust and feasible plan.

Table 10: Percent violations of budget constraints in different stages under different scenarios. A non-empty cell gives the yearly violations in that stage while the symbol '-' indicates that there is no violation in the corresponding year. An empty cell indicates that there is no violation in that stage.

Stage 2										6.11,6.76,6.17,4.87,5.15								
Stage 3														11.96,11.98,-,11.43,9.39				
Stage 4							1.25,1.42,1.44,1.40,-					1.25,1.42,1.44,1.40,-		1.25,1.42,1.44,1.40,-		11.32,12.23,12.36,12.18,-		
Stage 5								2.60,-,-,-,-					2.60,-,-,-,-		2.60,-,-,-,-		2.60,-,-,-,-	9.32,-,-,-,-
	FFFF	FFFS	FFSF	FFSS	FSFF	FSFS	FSSF	FSSS	SFFF	SFFS	SFSF	SFSS	SSFF	SSFS	SSSF	SSSS		

4.4.2. Comparison with Other Stochastic Models

To better understand the impact of scenarios on the optimal solution, we extend the scenario tree and solve the stochastic model using two extended versions. In the first version called the `3-by-2 Case`, we include 3 branches for BEB improvements at each stage (corresponding to Figure 1c) and 2 branches for HFCBs. The second version called the `2-by-3 Case` maintains 2 branches for BEBs and extends the number of HFCB branches to 3 (corresponding to Figure 2c). In both versions, the number of scenarios increases to $(1 \times 2 \times 3)^{5-1} = 1296$, making the problem size significantly larger complex. To manage this, we simplify certain assignment decisions. Specifically, for route-bus length pairs with higher demand in the winter schedule, assignment variables for other seasons are excluded. Instead, we assume that buses assigned to a cluster remain there across all seasons, with their usage adjusted based on seasonal demand, to account for lower O&M costs during other seasons. The detailed results are reported in the Supplementary Material.

We observe that in both extended cases the overall transition plan is similar to the `Base Case` as BEBs are still the dominant choice. However, in the Fast-Fast and Fast-Slow scenarios of the `3-by-2 Case`, the transition is nearly complete in year 14, as the Fast improvement branch of BEBs is faster in the `3-by-2 Case` than the `Base Case`. We also observe that HFCB purchases are almost identical in the `3-by-2 Case`

to the `Base Case`, meaning only a few buses being purchased in the final stage and under the Slow-Fast scenario, out of the 4 extreme scenarios. This is because the Slow improvement branch of BEBs in the `3-by-2 Case` is not much different than that of the Base Case.

The `2-by-3 Case` results are nearly identical to the `Base Case`. We observe that in the four extreme scenarios, only in the Slow-Fast scenario HFCBs are purchased, and the number of purchases is identical to the Slow-Fast scenario of the `Base Case`.

5. Conclusion

In this study, we propose a multi-stage stochastic program for the bus fleet replacement problem where we consider the uncertainties in the technology advancements and cost improvements of different bus technologies. We present a forecasting approach where we examine historical cost and efficiency trends of different technology options and compute the improvement ratios over the years. These ratios are then clustered into different groups which are provided to the multi-stage stochastic program as scenarios. We use our model to plan the transition of municipal bus network in Istanbul to clean alternatives (BEBs and HFCBs) over a planning horizon of 25 years with a zero-emission target in 2050. In our plan, we consider the changes in the energy consumption of BEBs on different routes and at different seasons, and we ensure operational feasibility by finding the diesel-electric replacement ratios and recharge scheduling for FC electric buses. We perform sensitivity analyses to test the effect of certain exogenously determined parameters and inputs on our results. We also compare our stochastic programming approach with a deterministic model, and show its advantage in providing feasible dynamic strategic transition plans.

Our results from the multi-stage stochastic program indicate that BEBs are viable alternatives to replace DBs to achieve zero emission bus fleet goals. BEBs can already satisfy the demand in most of the routes in Istanbul without the need to plan new bus lines or timetables even at today's technology level. Their lower O&M cost compared to DBs make them advantageous in the long term across all scenarios we implemented. Although DBs are needed to be purchased initially due to the old age of the fleet and higher investment costs of BEBs, as costs improve BEBs can replace all DBs and transition to an all-electric fleet can be completed in less than 20 years in most scenarios. The advantages of BEBs also manifest themselves in the sensitivity analyses we performed. When the available budget is higher, more BEBs are purchased accross all scenarios, proving that once initial investment barrier is overcome, BEBs are better alternatives to DBs over their lifetime. We also observe that under tighter emission constraints the number of BEBs increase only negligibly under most scenarios, showing BEBs are not only environmentally beneficial but also cost effective. We acknowledge that other adoption challenges such as potential need for grid investments, recharging scheduling and personnel training can pose certain barriers and slow down the transition in practice.

HFCBs do not prove to be preferable over BEBs across our scenarios- even under the most favorable scenario, less than 0.4% of the fleet consists of HFCBs. Higher investment and operational costs both play a role in this result. When the energy costs are decreased by one fifth, the fleet can consist of up to 24% of

HFCBs in the most favorable scenario but HFCBs still cannot be dominant due to their higher initial costs.

There are some limitations of our work that should be considered while interpreting our results. In this study, we assumed that the municipality is not responsible for building hydrogen transmission and storage infrastructure, or potential grid investments necessary for increased electricity demand. In a setting where the municipality has to invest in infrastructure, transition to cleaner alternatives might be slower. In addition, our results are based on scenarios obtained using limited historical HFCB cost and technological development trends compared to BEBs. According to these trends, even slow improvement in BEBs is faster than in HFCBs. However, our scenarios assume constant improvements based on past data and HFCBs are still at their early adoption stages being produced at limited numbers. It is possible that BEBs will reach a saturation in improvement sooner than HFCBs, which might change the results in favor of HFCBs in the future.

While this study focuses on strategical planning of the transition to zero emission buses, it can be enhanced by adding more tactical and operational aspects. For example, bus-to-route simulator might be improved by including recharge and maintenance scheduling optimization as well as battery degradation aspects. In our study, we assume each bus is changed with a bus of the same length, trip schedules do not change with transition and chargers are available at the last stop of every route when needed. Each of these assumptions pose an optimization problem by themselves: optimal bus size selection and assignment problem, optimizing trip schedules and charge location optimization. Our future work will focus on these problems and investigate how to integrate them into our model.

Finally, we will also investigate how to solve the large-scale multi-stage stochastic program more efficiently. This is especially important if one needs to include more technology options and construct larger technology trees that might provide a more realistic case study, albeit with a significantly larger scenario tree. In this case, obtaining structural results to systematically eliminate variables and constraints, and developing decomposition methods may prove to be necessary.

Acknowledgements

This work was supported by the Scientific and Technological Research Council of Turkey [grant number 222M243]. The authors thank IETT for providing detailed datasets related to the Istanbul public bus network, and Ahmet Emir Şener for his help related to Section 3.3.1.

References

Ajanovic, A., Glatt, A., & Haas, R. (2021). Prospects and impediments for hydrogen fuel cell buses. *Energy*, *235*, 121340. https://doi.org/10.1016/j.energy.2021.121340

An, K. (2020). Battery electric bus infrastructure planning under demand uncertainty. *Transportation Research Part C: Emerging Technologies*, *111*, 572–587. https://doi.org/10.1016/j.trc.2020.01.009

Anandarajah, G., McDowall, W., & Ekins, P. (2013). Decarbonising road transport with hydrogen and electricity: Long term global technology learning scenarios. *International Journal of Hydrogen Energy*, *38*(8), 3419–3432. https://doi.org/10.1016/j.ijhydene.2012.12.110

Autometris. (2023). Webplotdigitizer: A web-based tool to extract data from plots and graphs [Accessed: 2024-08-11]. https://automeris.io/

Benoliel, P., Jenn, A., & Tal, G. (2021). Examining energy uncertainty in battery bus deployments for transit agencies in california. *Transportation Research Part D: Transport and Environment*, *98*, 102963. https://doi.org/10.1016/j.trd.2021.102963

Bi, Z., De Kleine, R., & Keoleian, G. A. (2017). Integrated life cycle assessment and life cycle cost model for comparing plug-in versus wireless charging for an electric bus system. *Journal of Industrial Ecology*, *21*(2), 344–355. https://doi.org/10.1111/jiec.12419

Chen, Z., Yin, Y., & Song, Z. (2018). A cost-competitiveness analysis of charging infrastructure for electric bus operations. *Transportation Research Part C: Emerging Technologies*, *93*, 351–366. https://doi.org/10.1016/j.trc.2018.06.006

Collins, E., & Post, M. (2022, July). *Orange county transportation authority fuel cell electric bus progress report: Data period focus: Feb. 2020 through jul. 2021* (tech. rep.). National Renewable Energy Laboratory (NREL). https://www.nrel.gov/docs/fy22osti/83558.pdf

Dirks, N., Schiffer, M., & Walther, G. (2022). On the integration of battery electric buses into urban bus networks. *Transportation Research Part C: Emerging Technologies*, *139*, 103628. https://doi.org/10.1016/j.trc.2022.103628

Emiliano, W., Alvelos, F., Telhada, J., & Lanzer, E. A. (2020). An optimization model for bus fleet replacement with budgetary and environmental constraints. *Transportation Planning and Technology*, *43*(5), 488–502. https://doi.org/10.1080/03081060.2020.1763656

Encazip. (2024). Encazip website [Accessed: 2024-08-22]. https://www.encazip.com/elektrik-fiyatlari

European Commission. (2020). Sustainable and smart mobility strategy [Accessed: 2024-07-04]. https://transport.ec.europa.eu/transport-themes/mobility-strategy_en

Feng, W., & Figliozzi, M. (2014). Vehicle technologies and bus fleet replacement optimization: Problem properties and sensitivity analysis utilizing real-world data. *Public Transport*, *6*, 137–157. https://doi.org/10.1007/s12469-014-0086-z

Frieß, N. M., & Pferschy, U. (2024). Planning a zero-emission mixed-fleet public bus system with minimal life cycle cost. *Public Transport*, *16*(1), 39–79. https://doi.org/10.1007/s12469-023-00345-4

He, Y., Liu, Z., & Song, Z. (2022). Integrated charging infrastructure planning and charging scheduling for battery electric bus systems. *Transportation Research Part D: Transport and Environment*, *111*, 103437. https://doi.org/10.1016/j.trd.2022.103437

He, Y., Liu, Z., Zhang, Y., & Song, Z. (2023). Time-dependent electric bus and charging station deployment problem. *Energy*, *282*, 128227. https://doi.org/10.1016/j.energy.2023.128227

Holland, S. P., Mansur, E. T., Muller, N. Z., & Yates, A. J. (2021). The environmental benefits of transportation electrification: Urban buses. *Energy policy*, *148*, 111921. https://doi.org/10.1016/j.enpol.2020.111921

Huya-Kouadio, J., & James, B. D. (2023). *Fuel cell cost and performance analysis* (tech. rep.). United States Department of Energy.

IEA. (2023a). Net zero roadmap: A global pathway to keep the 1.5 °c goal in reach. *International Energy Agency*. https://www.iea.org/reports/net-zero-roadmap-a-global-pathway-to-keep-the-15-0c-goal-in-reach

IEA. (2023b). World energy outlook 2023. *International Energy Agency*. https://www.iea.org/reports/world-energy-outlook-2023

IEA. (2024a). Global EV outlook 2024. *International Energy Agency*. https://www.iea.org/reports/global-ev-outlook-2024

IEA. (2024b). Trucks and buses [Accessed: 2024-07-21]. *International Energy Agency*. https://www.iea.org/energy-system/transport/trucks-and-buses

IETT. (2023). İETT Faaliyet Raporu 2023. https://iett.istanbul/icerik/Raporlar

Islam, A., & Lownes, N. (2019). When to go electric? a parallel bus fleet replacement study. *Transportation Research Part D: Transport and Environment*, *72*, 299–311. https://doi.org/10.1016/j.trd.2019.05.007

Istanbul Metropolitan Municipality. (2022). Istanbul sustainable urban mobility plan (SUMP) [Accessed: 2024-07-22].

Keles, P., & Hartman, J. C. (2004). Case study: Bus fleet replacement. *The Engineering Economist*, *49*(3), 253–278. https://doi.org/10.1080/00137910490498951

Kunith, A., Mendelevitch, R., & Goehlich, D. (2017). Electrification of a city bus network—an optimization model for cost-effective placing of charging infrastructure and battery sizing of fast-charging electric bus systems. *International Journal of Sustainable Transportation*, *11*(10), 707–720. https://doi.org/10.1080/15568318.2017.1310962

Li, M., Tang, P., Lin, X., & He, F. (2022). Multistage planning of electric transit charging facilities under build-operate-transfer model. *Transportation Research Part D: Transport and Environment*, *102*, 103118. https://doi.org/10.1016/j.trd.2021.103118

Ma, X., Miao, R., Wu, X., & Liu, X. (2021). Examining influential factors on the energy consumption of electric and diesel buses: A data-driven analysis of large-scale public transit network in beijing. *Energy*, *216*, 119196. https://doi.org/10.1016/j.energy.2020.119196

Muratori, M., Kunz, T., Hula, A., Freedberg, M., et al. (2023). *Us national blueprint for transportation decarbonization: A joint strategy to transform transportation* (tech. rep.). United States. Department of Energy. Office of Energy Efficiency and ...

Open-Elevation API. (2020). Open-elevation website. https://open-elevation.com/

Pelletier, S., Jabali, O., Mendoza, J. E., & Laporte, G. (2019). The electric bus fleet transition problem. *Transportation Research Part C: Emerging Technologies*, *109*, 174–193. https://doi.org/10.1016/j.trc.2019.10.012

Perumal, S. S., Lusby, R. M., & Larsen, J. (2022). Electric bus planning & scheduling: A review of related problems and methodologies. *European Journal of Operational Research*, *301*(2), 395–413. https://doi.org/10.1016/j.ejor.2021.10.058.

Petrol Ofisi. (2024). Petrol ofisi website [Accessed: 2024-08-22]. https://www.petrolofisi.com.tr/arsiv-fiyatlari

Rogge, M., Van der Hurk, E., Larsen, A., & Sauer, D. U. (2018). Electric bus fleet size and mix problem with optimization of charging infrastructure. *Applied Energy*, *211*, 282–295. https://doi.org/10.1016/j.apenergy.2017.11.051

Shapiro, A., Dentcheva, D., & Ruszczynski, A. (2021). *Lectures on stochastic programming: Modeling and theory*. SIAM.

Shehabeldeen, A., Foda, A., & Mohamed, M. (2024). A multi-stage optimization of battery electric bus transit with battery degradation. *Energy*, *299*, 131359. https://doi.org/10.1016/j.energy.2024.131359

Stasko, T. H., & Gao, H. O. (2010). Reducing transit fleet emissions through vehicle retrofits, replacements, and usage changes over multiple time periods. *Transportation Research Part D: Transport and Environment*, *15*(5), 254–262. https://doi.org/10.1016/j.trd.2010.03.004

Tang, C., Li, X., Ceder, A., & Wang, X. (2021). Public transport fleet replacement optimization using multi-type battery-powered electric buses. *Transportation Research Record*, *2675*(12), 1422–1431. https://doi.org/10.1177/03611981211027157

Walter, D., Bond, K., Butler-Sloss, S., Speelman, L., Numata, Y., & Atkinson, W. (2023). X-change: Batteries, the battery domino effect.

Xylia, M., Leduc, S., Patrizio, P., Kraxner, F., & Silveira, S. (2017). Locating charging infrastructure for electric buses in Stockholm. *Transportation Research Part C: Emerging Technologies*, *78*, 183–200. https://doi.org/10.1016/j.trc.2017.03.005

Yıldırım, Ş., & Yıldız, B. (2021). Electric bus fleet composition and scheduling. *Transportation Research Part C: Emerging Technologies*, *129*, 103197. https://doi.org/10.1016/j.trc.2021.103197

Zhang, L., Liu, Z., Wang, W., & Yu, B. (2022). Long-term charging infrastructure deployment and bus fleet transition considering seasonal differences. *Transportation Research Part D: Transport and Environment*, *111*, 103429. https://doi.org/10.1016/j.trd.2022.103429

Zhou, Y., Ong, G. P., & Meng, Q. (2023). The road to electrification: Bus fleet replacement strategies. *Applied Energy*, *337*, 120903. https://doi.org/10.1016/j.apenergy.2023.120903

Appendix A. Energy Requirement Calculation

Appendix A.1. Determining the Segment Duration

To find τ_1 and τ_2, we can solve an optimization problem that minimizes the time spent within a segment of length d and a fixed acceleration a satisfying the condition that $V(\tau) \leq V_{\max}$ and

$$P_w(\tau) = \left(mg\sin(\alpha) + f_r mg\cos(\alpha) + 0.5\rho_{\text{air}} C_D A_f v(\tau)^2 + m_{\text{eq}} a(\tau)\right) v(\tau) \leq \min\{P_{\max}, \kappa V(\tau)\}$$

for $\tau \in [0, \tau_1 + \tau_2]$. To simplify, let us rewrite $P_w(\tau)$ as

$$P_w(\tau) = \left(A + Bv(\tau)^2 + Ca(\tau)\right) v(\tau).$$

Since the air resistance is much smaller than the other components (that is, $Bv(\tau)^2 \ll |A + Ca(\tau)|$ for the bus specifications and speed profiles we are interested in), we can formulate this optimization problem as follows when $\alpha > 0$ (for $\alpha < 0$, the power constraint is redundant):

$$\min\{\tau_1 + \tau_2 : a\tau_1 \leq V_{\max},\ a\tau_1\tau_2 = d,\ \tau_2 \geq \tau_1,\ P_w(\tau_1) \leq \min\{P_{\max}, \kappa a\tau_1)\}\}.$$

We can eliminate τ_2 by substituting $\frac{d}{a\tau_1}$:

$$\min\left\{\tau_1 + \frac{d}{a\tau_1} : a\tau_1 \leq V_{\max},\ \frac{d}{a\tau_1} \geq \tau_1,\ P_w(\tau_1) \leq P_{\max}, \tau \leq \sqrt{\frac{\kappa - A - Ca}{Ba^2}}\right\}.$$

Note that $\tau_1 + \frac{d}{a\tau_1}$ is a convex function with its minimizer at $\tau_1 = \sqrt{\frac{d}{a}}$. Since the cubic polynomial $P_w(\tau_1)$ is increasing under our assumptions, there exists a single root for $P_w(\tau_1) = P_{\max}$, which we denote by τ_R (note that we can search for that root in the interval $[0, \frac{V_{\max}}{a}]$). Finally, we conclude that the optimal solution is

$$\tau_1^* = \min\left\{\sqrt{\frac{d}{a}}, \frac{V_{\max}}{a}, \sqrt{\frac{\kappa - A - Ca}{Ba^2}}, \tau_R\right\} \text{ and } \tau_2^* = \frac{d}{a\tau_1^*}.$$

Appendix A.2. Calculating the Energy Consumption for BEBs

- In the acceleration phase, that is $\tau \in [0, \tau_1]$, we have $a(\tau) = a$, $v(\tau) = a\tau$, and we are interested in the following integral:
$$\int_0^{\tau_1} P_{\text{w}}(\tau) d\tau = \int_0^{\tau_1} (A + Ba^2\delta^2 + Ca) a\tau d\tau.$$

– If $A+Ca \geq 0$, we have

$$\int_0^{\tau_1} P_{\text{bat}}(\tau)d\tau = \frac{1}{\eta_t\eta_m}\int_0^{\tau_1} P_w(\tau)d\tau = \frac{1}{\eta_t\eta_m}\int_0^{\tau_1}\left(A+B(a\tau)^2+Ca\right)(a\tau)d\tau$$
$$= \frac{1}{\eta_t\eta_m}\left[\frac{1}{2}(A+Ca)a\tau_1^2+\frac{1}{4}Ba^3\tau_1^4\right].$$

– If $A+Ca<0$ and $\bar{\tau} := \sqrt{\frac{-(A+Ca)}{Ba^2}} \geq \tau_1$, we have

$$\int_0^{\tau_1} P_{\text{bat}}(\tau)d\tau = \eta_t\eta_m\eta_{rb}\int_0^{\tau_1} P_w(\tau)d\tau = \eta_t\eta_m\eta_{rb}\left[\frac{1}{2}(A+Ca)a\tau_1^2+\frac{1}{4}Ba^3\tau_1^4\right].$$

– If $A+Ca<0$ and $\bar{\tau} := \sqrt{\frac{-(A+Ca)}{Ba^2}} < \tau_1$, we have

$$\int_0^{\tau_1} P_{\text{bat}}(\tau)d\tau = \eta_t\eta_m\eta_{rb}\int_0^{\bar{\tau}}(A+Ba^2\delta^2+Ca)a\delta d\delta + \frac{1}{\eta_t\eta_m}\int_{\bar{\tau}}^{\tau_1}(A+Ba^2\delta^2+Ca)a\delta d\delta$$
$$= \eta_t\eta_m\eta_{rb}\left[\frac{1}{2}(A+Ca)a\bar{\tau}^2+\frac{1}{4}Ba^3\bar{\tau}^4\right]+\frac{1}{\eta_t\eta_m}\left[\frac{1}{2}(A+Ca)a(\tau_1^2-\bar{\tau}^2)+\frac{1}{4}Ba^3(\tau_1^4-\bar{\tau}^4)\right].$$

- In the constant speed phase, that is $\tau \in [\tau_1, \tau_2]$, we have $a(\tau)=0$ and $v(\tau)=a\tau_1$, and we are interested in the following integral:

$$\int_{\tau_1}^{\tau_2} P_w(\tau)d\tau = \int_{\tau_1}^{\tau_2}\left(A+B(a\tau_1)^2\right)(a\tau_1)d\tau = \left(A+B(a\tau_1)^2\right)(a\tau_1)(\tau_2-\tau_1) =: \mathscr{C}.$$

– If $\mathscr{C} \geq 0$, we have

$$\int_{\tau_1}^{\tau_2} P_{\text{bat}}(\tau)d\tau = \frac{1}{\eta_t\eta_m}\int_{\tau_1}^{\tau_2} P_w(\tau)d\tau = \frac{1}{\eta_t\eta_m}\mathscr{C}.$$

– If $\mathscr{C} < 0$, we have

$$\int_{\tau_1}^{\tau_2} P_{\text{bat}}(\tau)d\tau = \eta_t\eta_m\eta_{rb}\int_{\tau_1}^{\tau_2} P_w(\tau)d\tau = \eta_t\eta_m\eta_{rb}\mathscr{C}.$$

- In the deceleration phase, that is $\tau \in [\tau_2, \tau_1+\tau_2]$, we have $a(\tau)=-a$ and $v(\tau)=a(\tau_1+\tau_2-t)$. Let us first apply change of variables $\delta = \tau_1+\tau_2-\tau$ so that we are interested in the following integral:

$$\int_{\tau_2}^{\tau_1+\tau_2} P_{\text{w}}(\tau)d\tau = \int_0^{\tau_1} P_{\text{w}}(\tau_1+\tau_2-\delta)d\delta = \int_0^{\tau_1}(A+Ba^2\delta^2-Ca)a\delta d\delta.$$

– If $A-Ca \geq 0$, we have

$$\int_{\tau_2}^{\tau_1+\tau_2} P_{\text{bat}}(\tau)d\tau = \frac{1}{\eta_t\eta_m}\int_0^{\tau_1}(A+Ba^2\delta^2-Ca)a\delta d\delta = \frac{1}{\eta_t\eta_m}\left[\frac{1}{2}(A-Ca)a\tau_1^2+\frac{1}{4}Ba^3\tau_1^4\right].$$

– If $A - Ca < 0$ and $\bar{\delta} := \sqrt{\frac{Ca-A}{Ba^2}} \geq \tau_1$, we have

$$\int_{\tau_2}^{\tau_1+\tau_2} P_{\text{bat}}(\tau)d\tau = \eta_t \eta_m \eta_{rb} \int_0^{\tau_1} (A + Ba^2\delta^2 - Ca)a\delta d\delta = \eta_t \eta_m \eta_{rb} \left[\frac{1}{2}(A-Ca)a\tau_1^2 + \frac{1}{4}Ba^3\tau_1^4\right].$$

– If $A - Ca < 0$ and $\bar{\delta} := \sqrt{\frac{Ca-A}{Ba^2}} < \tau_1$, we have

$$\begin{aligned}\int_{\tau_2}^{\tau_1+\tau_2} P_{\text{bat}}(\tau)d\tau &= \eta_t \eta_m \eta_{rb} \int_0^{\bar{\delta}} (A + Ba^2\delta^2 - Ca)a\delta d\delta + \frac{1}{\eta_t \eta_m} \int_{\bar{\delta}}^{\tau_1} (A + Ba^2\delta^2 - Ca)a\delta d\delta \\ &= \eta_t \eta_m \eta_{rb} \left[\frac{1}{2}(A-Ca)a\bar{\delta}^2 + \frac{1}{4}Ba^3\bar{\delta}^4\right] + \frac{1}{\eta_t \eta_m} \left[\frac{1}{2}(A-Ca)a(\tau_1^2 - \bar{\delta}^2) + \frac{1}{4}Ba^3(\tau_1^4 - \bar{\delta}^4)\right].\end{aligned}$$

For the energy requirement calculations, we use the parameters listed in Table A.11 for BEBs. Vehicle mass m includes the body mass m_{body} and the energy capacity multiplied with the unit battery mass m_{bat}.

Table A.11: List of parameters for traction power and battery power calculations (acceleration and vehicle body mass are given for 8, 10, 12, 18 m bus groups, respectively).

Parameter	**Value**	**Parameter**	**Value**
f_r	0.01	ρ_{air}	1.225 kg/m^3
C_D	0.7	g	9.81 m/s^2
A_f	$0.85 \times 3.25 \times 2.55 = 7.04$m^2	η_t	0.9
η_m	0.9	η_{rb}	0.25
m_{body}	9.5, 15, 16, 25 tonnes	m_{bat}	5 kg/kWh
m_{eq}	$1.1 \times m$	a	2.1, 1.8, 1.7, 1.5 m/s^2

Appendix B. Data

Appendix B.1. IETT Data Details

Here is a snapshot of the “Trip Schedule" dataset:

Day	Route Code	Route Name	Trip ID	Scheduled Start Time	Planned Km	Vehicle Depot	Vehicle Length Group (m)
15.03.2023	129T	BOSTANCI - TAKSİM	129T_D_D0	15.03.2023 08:00:00	19.37409	ÖHO	11-14
15.03.2023	129T	BOSTANCI - TAKSİM	129T_G_D0	15.03.2023 09:30:00	22.8153	ÖHO	11-14
15.03.2023	129T	BOSTANCI - TAKSİM	129T_D_D0	15.03.2023 11:00:00	19.37409	ÖHO	11-14
15.03.2023	129T	BOSTANCI - TAKSİM	129T_G_D0	15.03.2023 13:00:00	22.8153	ÖHO	11-14

Figure B.9: Snapshot of the “Trip Schedule" dataset.

Summary statistics of the “Trip Schedule" dataset are provided in Table B.12.

Table B.12: Trip schedule summaries for March 15 and August 3, 2023. On March 15, service trips were planned for 2,863 route types with a total of 13,467 different bus stops visited, while on August 3, services were planned for 2,704 route types with 13,501 different bus stops visited.

Bus Length Group (m)	**Summer Schedule (August 3, 2023)**			**Winter Schedule (March 15, 2023)**		
	Total Planned Services	**Total Planned Distance** (km)	**Total Assigned Routes**	**Total Planned Services**	**Total Planned Distance** (km)	**Total Assigned Routes**
6.5-8	2,898	63,525	38	2,948	61,200	37
8-9	277	4,320	14	275	4,308	14
10-11	76	3,086	8	64	2,635	6
11-14	35,761	823,868	738	36,578	853,222	736
11-14 natural gas	1,464	26,448	129	1,554	30,263	145
14-19	7,727	274,523	79	9,130	317,813	98
Total	**48,203**	**1,192,684**	**820**	**50,549**	**1,269,441**	**819**

Here is a snapshot of the “Stop Sequence with Coordinates" dataset:

Route Code	Trip ID	Stop Name	Stop ID	Stop Type	X Coordinate	Y Coordinate	Sequence	Haversine Distance (km)	Elevation (m)
129T	129T_D_D0	GÜMÜŞSUYU PERON	301421	WALLMODERN	28.98936272	41.03986358	1	-	76
129T	129T_D_D0	GÜMÜŞSUYU	117382	İETTBAYRAK	28.991199	41.039178	2	0.171842796	51
129T	129T_D_D0	MİMAR SİNAN ÜNİVERSİTESİ	184932	İETTBAYRAK	29.00111964	41.04067353	3	0.848490852	9
129T	129T_D_D0	DENİZ MÜZESİ	184091	WALLMODERN	29.00654803	41.04190763	4	0.475496587	11

Figure B.10: Snapshot of the “Stop Sequence with Coordinates” dataset.

Appendix B.2. Technological Change

Appendix B.2.1. BEB Technological Change

Table B.13: Technological change for BEBs over the years (energy density is given in Wh/kg and battery cell cost is given wrt 2023 USD/kWh).

Year	Energy Density	Cost	Year	Energy Density	Cost	Year	Energy Density	Cost
1991	98.20	8805.20	2002	188.18	1327.70	2013	243.23	472.73
1992	102.75	7166.22	2003	193.37	1014.27	2014	251.54	409.52
1993	107.86	5756.38	2004	209.99	909.97	2015	248.43	280.86
1994	112.98	6451.60	2005	202.72	788.02	2016	259.85	235.02
1995	118.66	6068.66	2006	207.92	675.05	2017	276.47	170.31
1996	126.62	5151.87	2007	222.46	644.22	2018	293.09	142.60
1997	130.59	4398.27	2008	218.30	673.49	2019	313.87	119.58
1998	144.80	3541.91	2009	222.46	580.73	2020	334.64	111.57
1999	156.37	2741.66	2010	230.77	533.49	2021	389.70	107.44
2000	160.13	2576.53	2011	238.04	499.68	2022	444.75	119.23
2001	179.87	1832.35	2012	243.23	507.12	2023	499.80	100.63

Table B.14: Clustering results for BEBs.

Clusters	Cluster Probability	Energy Density Improvement Rate	Cost Improvement Rate	Energy Density Change	Cost Change
2 Clusters	**F** (0.46)	0.27	1.05	1.31	0.35
	S (0.54)	0.19	0.45	1.21	0.63
3 Clusters	**F** (0.32)	0.25	1.14	1.28	0.32
	M (0.25)	0.24	0.79	1.27	0.45
	S (0.429)	0.21	0.39	1.24	0.68

Appendix B.2.2. HFCB Technological Change

Table B.15: Technological change for HFCBs over the years (fuel cell system cost is given wrt 2016 USD/kW).

Year	Efficiency	Cost	Year	Efficiency	Cost	Year	Efficiency	Cost
2010		175	2015		99	2020	0.57	76
2011		142	2016		99	2021	0.57	
2012	0.50	122	2017	0.55	78	2022		71
2013	0.50	119	2018		79	2023	0.57	
2014		107	2019		79	2024	0.60	

Table B.16: Clustering results for HFCBs.

Clusters	Cluster Probability	Efficiency Improvement Rate	Cost Improvement Rate	Efficiency Change	Cost Change
2 Clusters	**F** (0.83)	0.09	0.35	1.09	0.71
	S (0.17)	0.04	0.09	1.04	0.91
3 Clusters	**F** (0.33)	0.10	0.43	1.11	0.65
	M (0.50)	0.08	0.29	1.08	0.75
	S (0.17)	0.04	0.09	1.04	0.91

Appendix B.3. Scenario Table

Table B.17 shows the technological improvements across different stages of each scenario, along with the scenario's probability (in percent). The columns labeled S2, S3, S4, and S5 refer to stages 2, 3, 4, and 5, respectively. In each stage, the first letter represents the BEB improvement, and the second letter refers to the HFCB improvement. For example, "FS" means that BEBs improve fast, while HFCBs improve slow.

ID	S2	S3	S4	S5	Prob. (%)	ID	S2	S3	S4	S5	Prob. (%)	ID	S2	S3	S4	S5	Prob. (%)	ID	S2	S3	S4	S5	Prob. (%)
1	FF	FF	FF	FF	2.12493	65	FS	FF	FF	FF	0.43523	129	SF	FF	FF	FF	2.49448	193	SS	FF	FF	FF	0.51092
2	FF	FF	FF	FS	0.43523	66	FS	FF	FF	FS	0.08914	130	SF	FF	FF	FS	0.51092	194	SS	FF	FF	FS	0.10465
3	FF	FF	FF	SF	2.49448	67	FS	FF	FF	SF	0.51092	131	SF	FF	FF	SF	2.92830	195	SS	FF	FF	SF	0.59977
4	FF	FF	FF	SS	0.51092	68	FS	FF	FF	SS	0.10465	132	SF	FF	FF	SS	0.59977	196	SS	FF	FF	SS	0.12284
5	FF	FF	FS	FF	0.43523	69	FS	FF	FS	FF	0.08914	133	SF	FF	FS	FF	0.51092	197	SS	FF	FS	FF	0.10465
6	FF	FF	FS	FS	0.08914	70	FS	FF	FS	FS	0.01826	134	SF	FF	FS	FS	0.10465	198	SS	FF	FS	FS	0.02143
7	FF	FF	FS	SF	0.51092	71	FS	FF	FS	SF	0.10465	135	SF	FF	FS	SF	0.59977	199	SS	FF	FS	SF	0.12284
8	FF	FF	FS	SS	0.10465	72	FS	FF	FS	SS	0.02143	136	SF	FF	FS	SS	0.12284	200	SS	FF	FS	SS	0.02516
9	FF	FF	SF	FF	2.49448	73	FS	FF	SF	FF	0.51092	137	SF	FF	SF	FF	2.92830	201	SS	FF	SF	FF	0.59977
10	FF	FF	SF	FS	0.51092	74	FS	FF	SF	FS	0.10465	138	SF	FF	SF	FS	0.59977	202	SS	FF	SF	FS	0.12284
11	FF	FF	SF	SF	2.92830	75	FS	FF	SF	SF	0.59977	139	SF	FF	SF	SF	3.43757	203	SS	FF	SF	SF	0.70408
12	FF	FF	SF	SS	0.59977	76	FS	FF	SF	SS	0.12284	140	SF	FF	SF	SS	0.70408	204	SS	FF	SF	SS	0.14421
13	FF	FF	SS	FF	0.51092	77	FS	FF	SS	FF	0.10465	141	SF	FF	SS	FF	0.59977	205	SS	FF	SS	FF	0.12284
14	FF	FF	SS	FS	0.10465	78	FS	FF	SS	FS	0.02143	142	SF	FF	SS	FS	0.12284	206	SS	FF	SS	FS	0.02516
15	FF	FF	SS	SF	0.59977	79	FS	FF	SS	SF	0.12284	143	SF	FF	SS	SF	0.70408	207	SS	FF	SS	SF	0.14421
16	FF	FF	SS	SS	0.12284	80	FS	FF	SS	SS	0.02516	144	SF	FF	SS	SS	0.14421	208	SS	FF	SS	SS	0.02954
17	FF	FS	FF	FF	0.43523	81	FS	FS	FF	FF	0.08914	145	SF	FS	FF	FF	0.51092	209	SS	FS	FF	FF	0.10465
18	FF	FS	FF	FS	0.08914	82	FS	FS	FF	FS	0.01826	146	SF	FS	FF	FS	0.10465	210	SS	FS	FF	FS	0.02143
19	FF	FS	FF	SF	0.51092	83	FS	FS	FF	SF	0.10465	147	SF	FS	FF	SF	0.59977	211	SS	FS	FF	SF	0.12284
20	FF	FS	FF	SS	0.10465	84	FS	FS	FF	SS	0.02143	148	SF	FS	FF	SS	0.12284	212	SS	FS	FF	SS	0.02516
21	FF	FS	FS	FF	0.08914	85	FS	FS	FS	FF	0.01826	149	SF	FS	FS	FF	0.10465	213	SS	FS	FS	FF	0.02143
22	FF	FS	FS	FS	0.01826	86	FS	FS	FS	FS	0.00374	150	SF	FS	FS	FS	0.02143	214	SS	FS	FS	FS	0.00439
23	FF	FS	FS	SF	0.10465	87	FS	FS	FS	SF	0.02143	151	SF	FS	FS	SF	0.12284	215	SS	FS	FS	SF	0.02516
24	FF	FS	FS	SS	0.02143	88	FS	FS	FS	SS	0.00439	152	SF	FS	FS	SS	0.02516	216	SS	FS	FS	SS	0.00515
25	FF	FS	SF	FF	0.51092	89	FS	FS	SF	FF	0.10465	153	SF	FS	SF	FF	0.59977	217	SS	FS	SF	FF	0.12284
26	FF	FS	SF	FS	0.10465	90	FS	FS	SF	FS	0.02143	154	SF	FS	SF	FS	0.12284	218	SS	FS	SF	FS	0.02516
27	FF	FS	SF	SF	0.59977	91	FS	FS	SF	SF	0.12284	155	SF	FS	SF	SF	0.70408	219	SS	FS	SF	SF	0.14421
28	FF	FS	SF	SS	0.12284	92	FS	FS	SF	SS	0.02516	156	SF	FS	SF	SS	0.14421	220	SS	FS	SF	SS	0.02954
29	FF	FS	SS	FF	0.10465	93	FS	FS	SS	FF	0.02143	157	SF	FS	SS	FF	0.12284	221	SS	FS	SS	FF	0.02516
30	FF	FS	SS	FS	0.02143	94	FS	FS	SS	FS	0.00439	158	SF	FS	SS	FS	0.02516	222	SS	FS	SS	FS	0.00515
31	FF	FS	SS	SF	0.12284	95	FS	FS	SS	SF	0.02516	159	SF	FS	SS	SF	0.14421	223	SS	FS	SS	SF	0.02954
32	FF	FS	SS	SS	0.02516	96	FS	FS	SS	SS	0.00515	160	SF	FS	SS	SS	0.02954	224	SS	FS	SS	SS	0.00605
33	FF	SF	FF	FF	2.49448	97	FS	SF	FF	FF	0.51092	161	SF	SF	FF	FF	2.92830	225	SS	SF	FF	FF	0.59977
34	FF	SF	FF	FS	0.51092	98	FS	SF	FF	FS	0.10465	162	SF	SF	FF	FS	0.59977	226	SS	SF	FF	FS	0.12284
35	FF	SF	FF	SF	2.92830	99	FS	SF	FF	SF	0.59977	163	SF	SF	FF	SF	3.43757	227	SS	SF	FF	SF	0.70408
36	FF	SF	FF	SS	0.59977	100	FS	SF	FF	SS	0.12284	164	SF	SF	FF	SS	0.70408	228	SS	SF	FF	SS	0.14421
37	FF	SF	FS	FF	0.51092	101	FS	SF	FS	FF	0.10465	165	SF	SF	FS	FF	0.59977	229	SS	SF	FS	FF	0.12284
38	FF	SF	FS	FS	0.10465	102	FS	SF	FS	FS	0.02143	166	SF	SF	FS	FS	0.12284	230	SS	SF	FS	FS	0.02516
39	FF	SF	FS	SF	0.59977	103	FS	SF	FS	SF	0.12284	167	SF	SF	FS	SF	0.70408	231	SS	SF	FS	SF	0.14421
40	FF	SF	FS	SS	0.12284	104	FS	SF	FS	SS	0.02516	168	SF	SF	FS	SS	0.14421	232	SS	SF	FS	SS	0.02954
41	FF	SF	SF	FF	2.92830	105	FS	SF	SF	FF	0.59977	169	SF	SF	SF	FF	3.43757	233	SS	SF	SF	FF	0.70408
42	FF	SF	SF	FS	0.59977	106	FS	SF	SF	FS	0.12284	170	SF	SF	SF	FS	0.70408	234	SS	SF	SF	FS	0.14421
43	FF	SF	SF	SF	3.43757	107	FS	SF	SF	SF	0.70408	171	SF	SF	SF	SF	4.03541	235	SS	SF	SF	SF	0.82653
44	FF	SF	SF	SS	0.70408	108	FS	SF	SF	SS	0.14421	172	SF	SF	SF	SS	0.82653	236	SS	SF	SF	SS	0.16929
45	FF	SF	SS	FF	0.59977	109	FS	SF	SS	FF	0.12284	173	SF	SF	SS	FF	0.70408	237	SS	SF	SS	FF	0.14421
46	FF	SF	SS	FS	0.12284	110	FS	SF	SS	FS	0.02516	174	SF	SF	SS	FS	0.14421	238	SS	SF	SS	FS	0.02954
47	FF	SF	SS	SF	0.70408	111	FS	SF	SS	SF	0.14421	175	SF	SF	SS	SF	0.82653	239	SS	SF	SS	SF	0.16929
48	FF	SF	SS	SS	0.14421	112	FS	SF	SS	SS	0.02954	176	SF	SF	SS	SS	0.16929	240	SS	SF	SS	SS	0.03467
49	FF	SS	FF	FF	0.51092	113	FS	SS	FF	FF	0.10465	177	SF	SS	FF	FF	0.59977	241	SS	SS	FF	FF	0.12284
50	FF	SS	FF	FS	0.10465	114	FS	SS	FF	FS	0.02143	178	SF	SS	FF	FS	0.12284	242	SS	SS	FF	FS	0.02516
51	FF	SS	FF	SF	0.59977	115	FS	SS	FF	SF	0.12284	179	SF	SS	FF	SF	0.70408	243	SS	SS	FF	SF	0.14421
52	FF	SS	FF	SS	0.12284	116	FS	SS	FF	SS	0.02516	180	SF	SS	FF	SS	0.14421	244	SS	SS	FF	SS	0.02954
53	FF	SS	FS	FF	0.10465	117	FS	SS	FS	FF	0.02143	181	SF	SS	FS	FF	0.12284	245	SS	SS	FS	FF	0.02516
54	FF	SS	FS	FS	0.02143	118	FS	SS	FS	FS	0.00439	182	SF	SS	FS	FS	0.02516	246	SS	SS	FS	FS	0.00515
55	FF	SS	FS	SF	0.12284	119	FS	SS	FS	SF	0.02516	183	SF	SS	FS	SF	0.14421	247	SS	SS	FS	SF	0.02954
56	FF	SS	FS	SS	0.02516	120	FS	SS	FS	SS	0.00515	184	SF	SS	FS	SS	0.02954	248	SS	SS	FS	SS	0.00605
57	FF	SS	SF	FF	0.59977	121	FS	SS	SF	FF	0.12284	185	SF	SS	SF	FF	0.70408	249	SS	SS	SF	FF	0.14421
58	FF	SS	SF	FS	0.12284	122	FS	SS	SF	FS	0.02516	186	SF	SS	SF	FS	0.14421	250	SS	SS	SF	FS	0.02954
59	FF	SS	SF	SF	0.70408	123	FS	SS	SF	SF	0.14421	187	SF	SS	SF	SF	0.82653	251	SS	SS	SF	SF	0.16929
60	FF	SS	SF	SS	0.14421	124	FS	SS	SF	SS	0.02954	188	SF	SS	SF	SS	0.16929	252	SS	SS	SF	SS	0.03467
61	FF	SS	SS	FF	0.12284	125	FS	SS	SS	FF	0.02516	189	SF	SS	SS	FF	0.14421	253	SS	SS	SS	FF	0.02954
62	FF	SS	SS	FS	0.02516	126	FS	SS	SS	FS	0.00515	190	SF	SS	SS	FS	0.02954	254	SS	SS	SS	FS	0.00605
63	FF	SS	SS	SF	0.14421	127	FS	SS	SS	SF	0.02954	191	SF	SS	SS	SF	0.16929	255	SS	SS	SS	SF	0.03467
64	FF	SS	SS	SS	0.02954	128	FS	SS	SS	SS	0.00605	192	SF	SS	SS	SS	0.03467	256	SS	SS	SS	SS	0.00710

Table B.17: Scenario Table

Appendix C. Detailed Results of the Sensitivity Analysis

Appendix C.1. Relaxed Budget

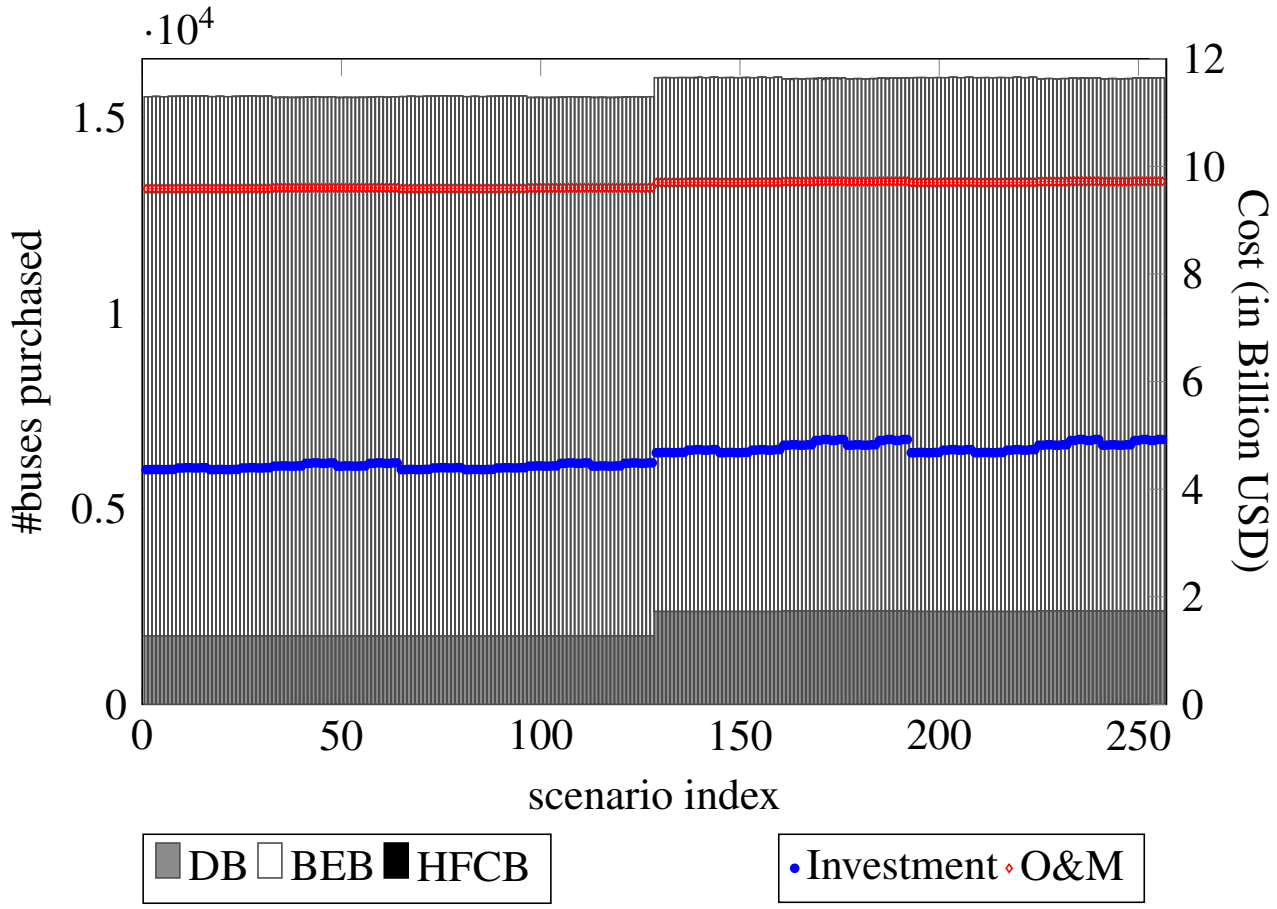

Figure C.11: Relaxed Budget

Figure C.11 represents the case where the annual budget is set at 300 million USD. The optimization process took 5,888 seconds, resulting in an objective function value of 13,586,698,671 USD. After rounding the variables, the objective function value increased to 13,615,884,770 USD.

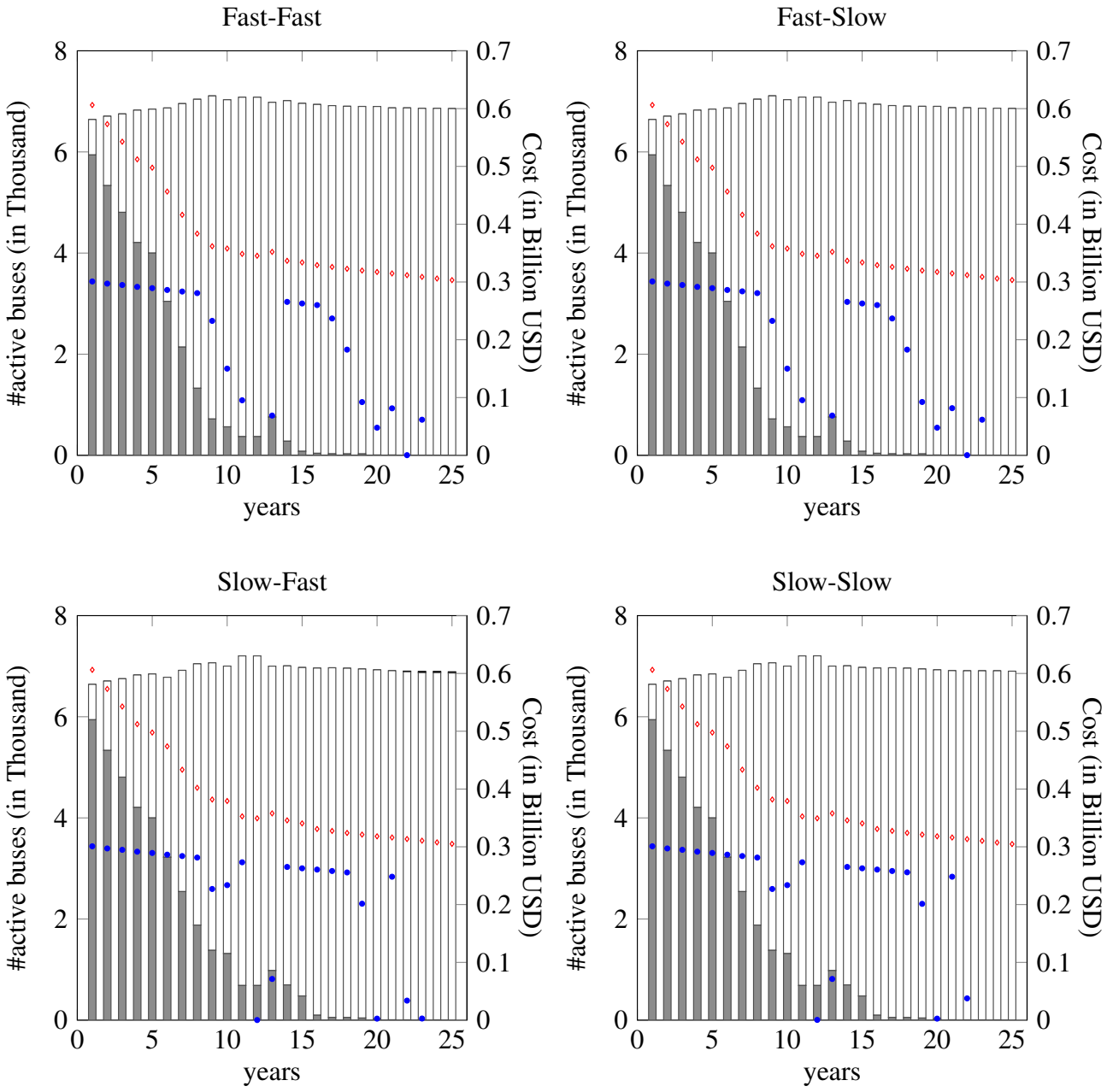

Figure C.12: Relaxed Budget -four specific scenarios.

Appendix C.2. Strict Emission Constraints

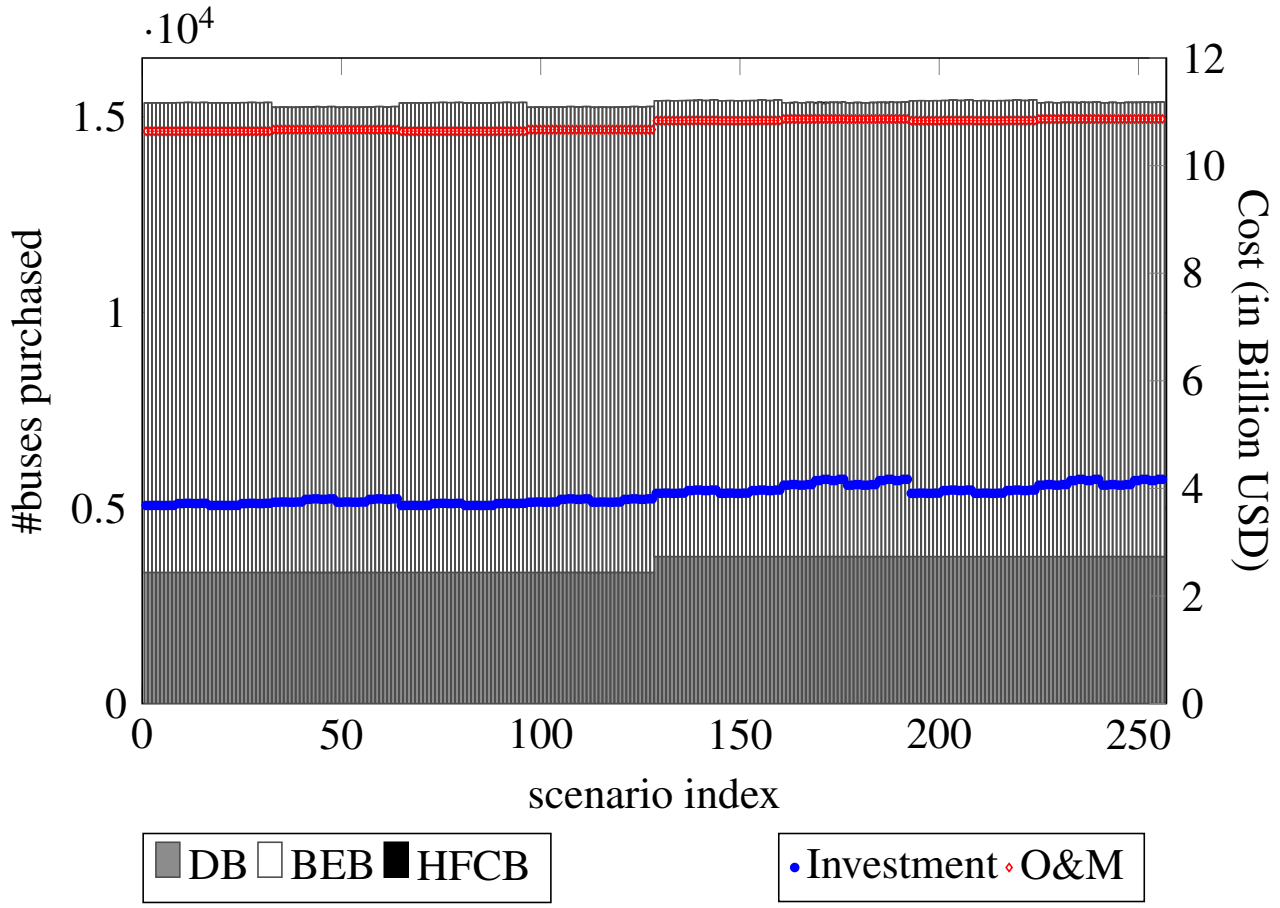

Figure C.13: Strict Emission Constraints

Figure C.13 represents the case with only zero emission limits in the final period, and without any intermediate targets. The optimization process took 4,877 seconds, resulting in an objective function value of 14,133,211,491 USD. After rounding the variables, the objective function value increased to 14,165,320,512 USD.

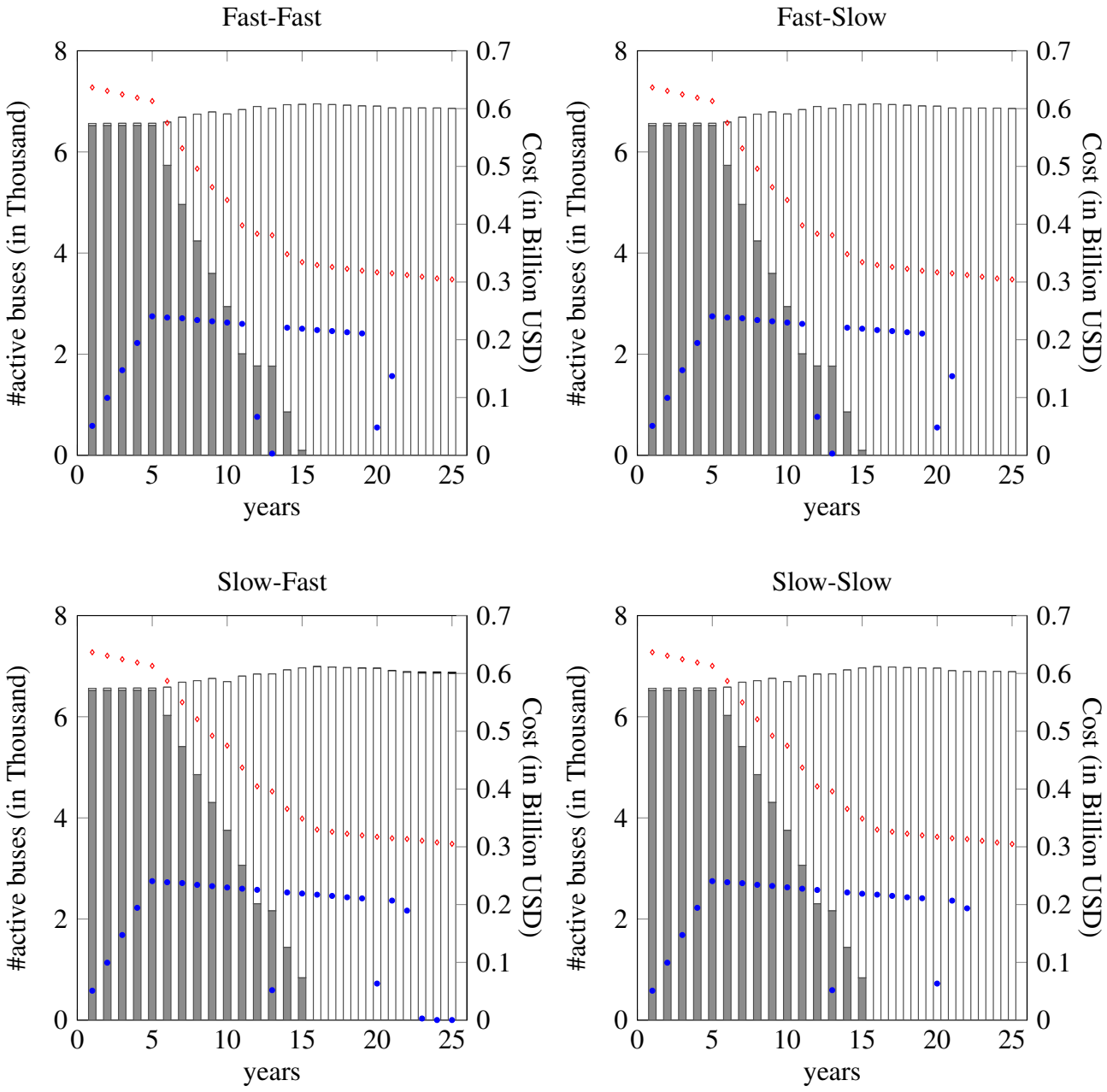

Figure C.14: Strict Emission Constraints

Appendix C.3. Reduced Hydrogen Price

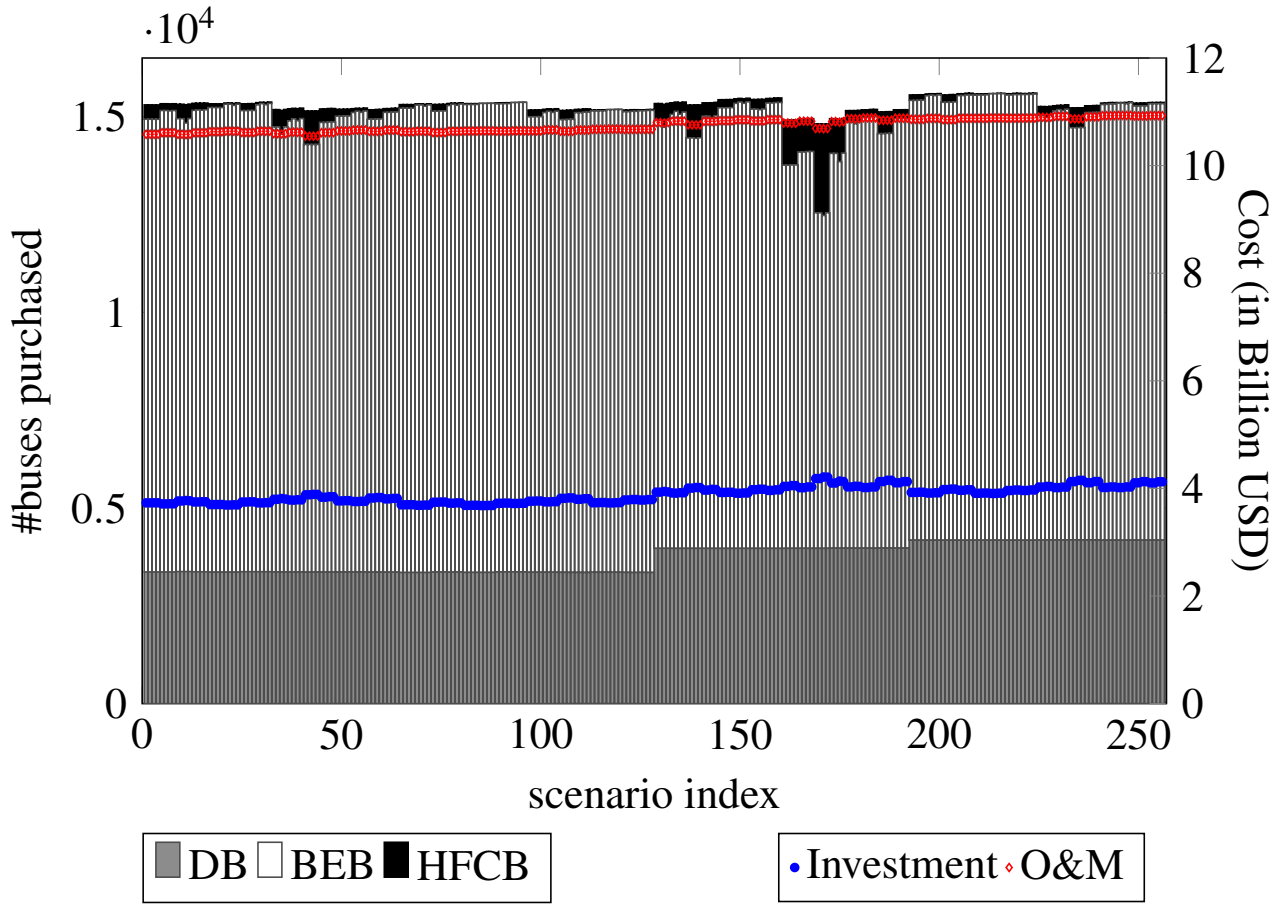

Figure C.15: Reduced Hydrogen Price

Figure C.15 represents the case where hydrogen price is reduced to 2 USD per kg. The optimization process took 6,133 seconds, resulting in an objective function value of 14,099,073,373 USD. After rounding the variables, the objective function value increased to 14,129,697,437 USD.

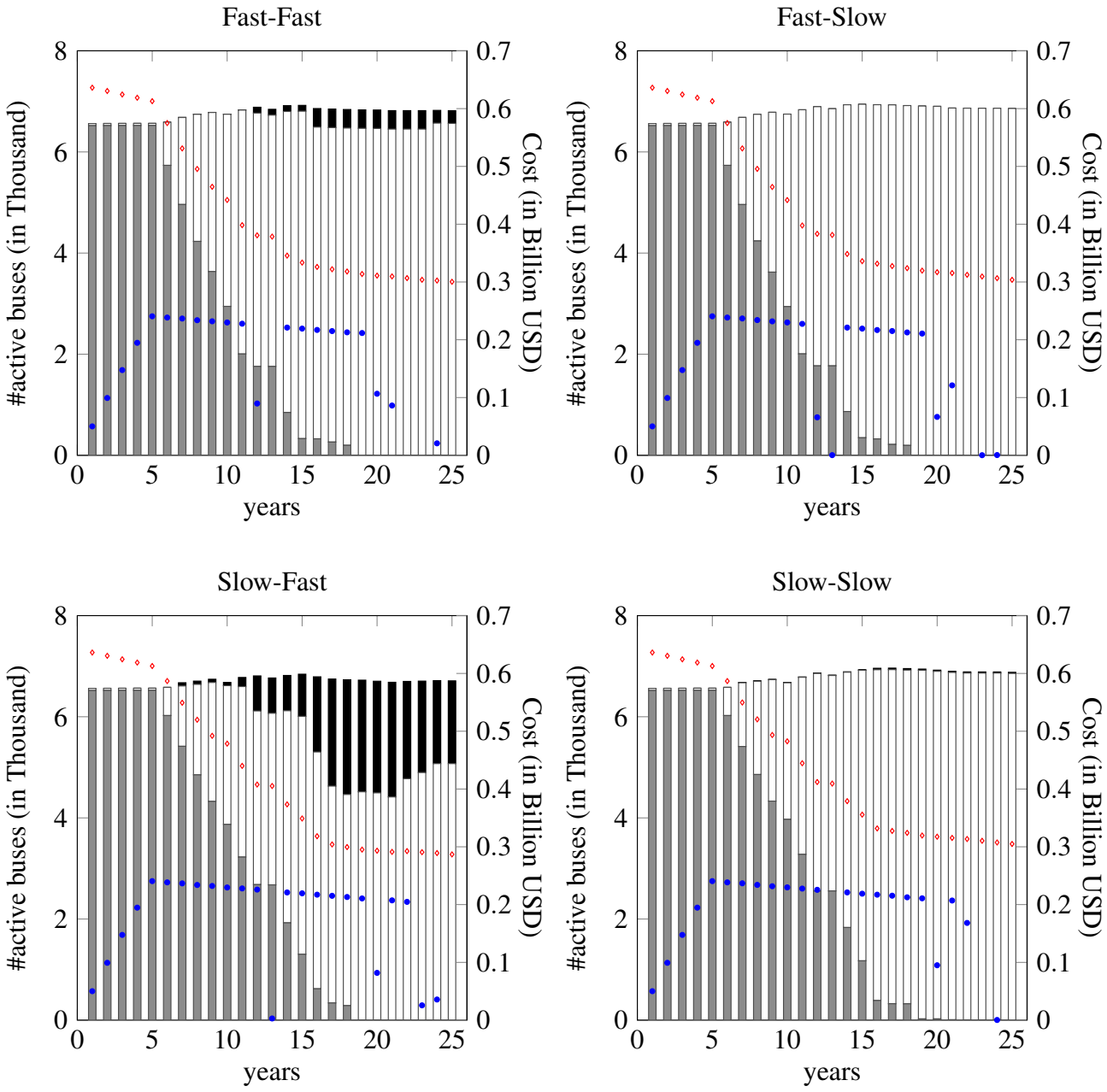

Figure C.16: Reduced Hydrogen Price

Appendix D. Detailed Results of Model Comparison

Appendix D.1. Base Case - Simplified Assignments

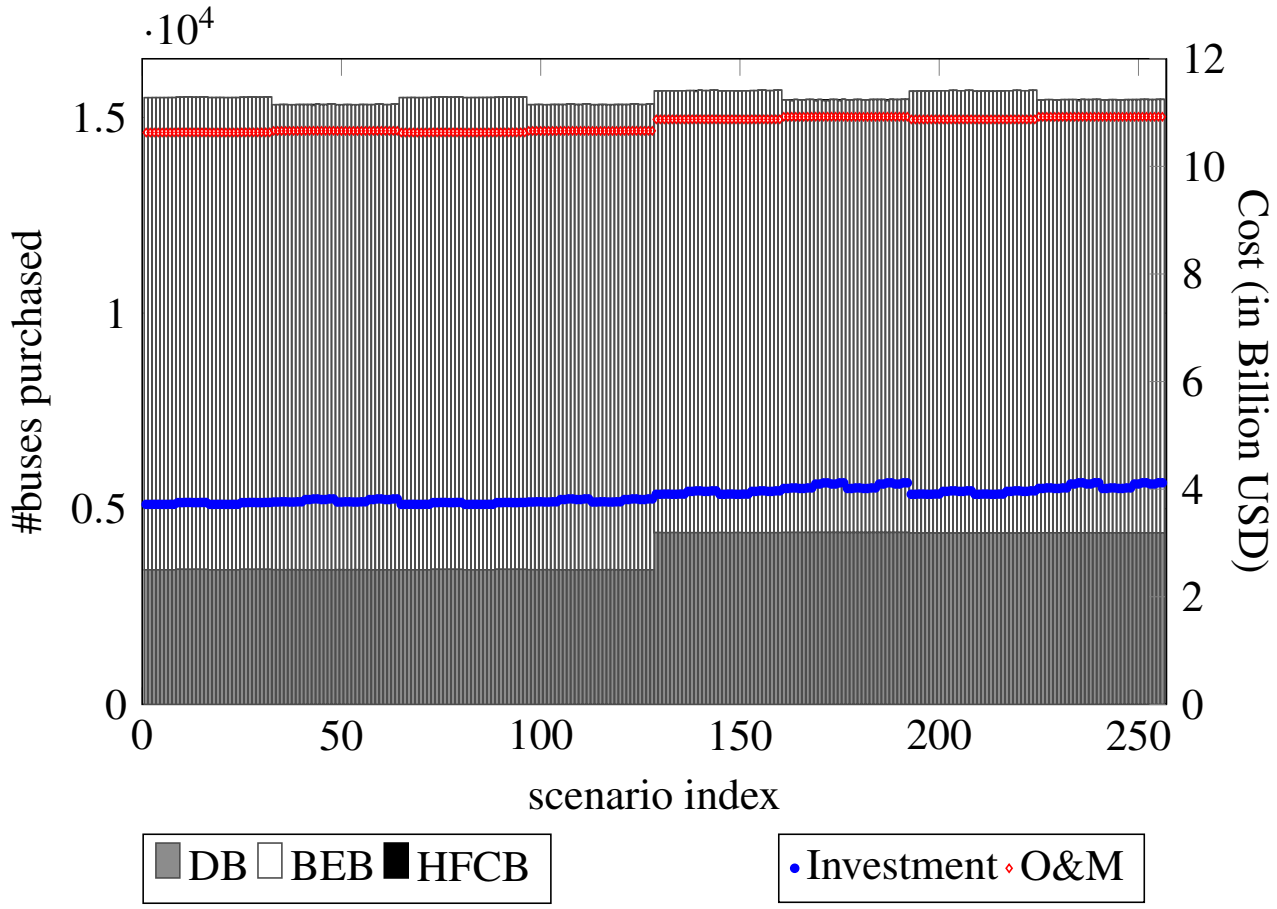

Figure D.17: Base Case with Simplified Assignments

Figure D.17 represents the simplified assignments version of the Base Case. In this case, we assume that for route-bus length pairs with a higher demand in the winter, the buses assigned to a cluster will remain in that cluster on all other seasons. However, we adjust the O&M costs based on the seasonal difference in demand. The optimization process took 1,770 seconds, resulting in an objective function value of 14,111,317,685 USD. After rounding the variables, the objective function value increased to 14,136,930,170 USD.

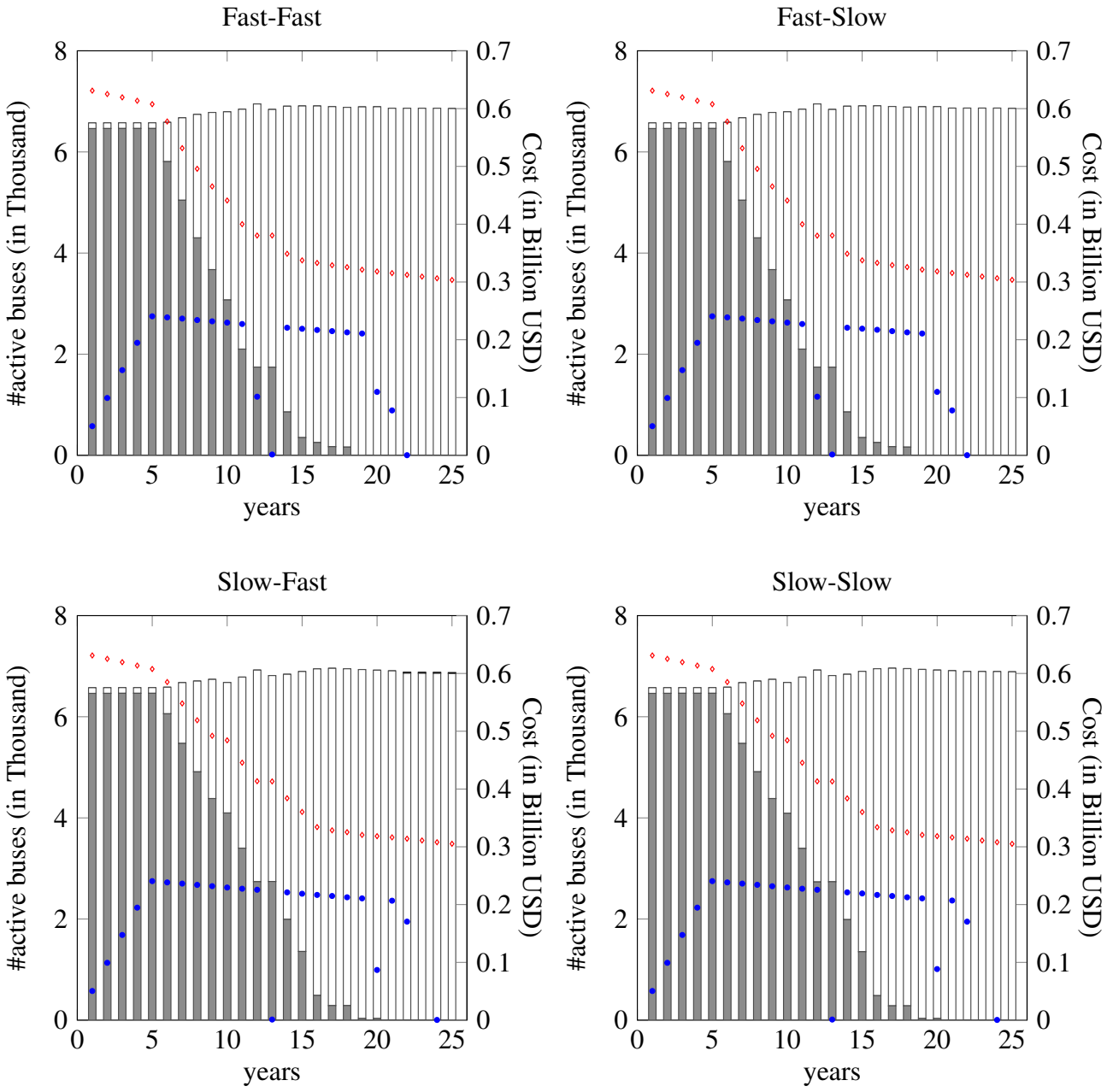

Figure D.18: Base Case - Simplified Assignments

Appendix D.2. Extended Scenario Tree - 3 By 2

We present the results of the Extended Scenario Tree - 3 By 2 case in Figure D.19. In this case, three branches for BEB technological improvements and 2 branches for HFCB technological improvements are considered in each stage. Similar to Appendix D.1, we simplify the assignment decisions for route-bus length combinations having higher demand in the winter. CPU time is 17,673 seconds, the total expected costs is 13,265,506,356 USD, which increases to 13,288,586,164 USD after rounding the variables.

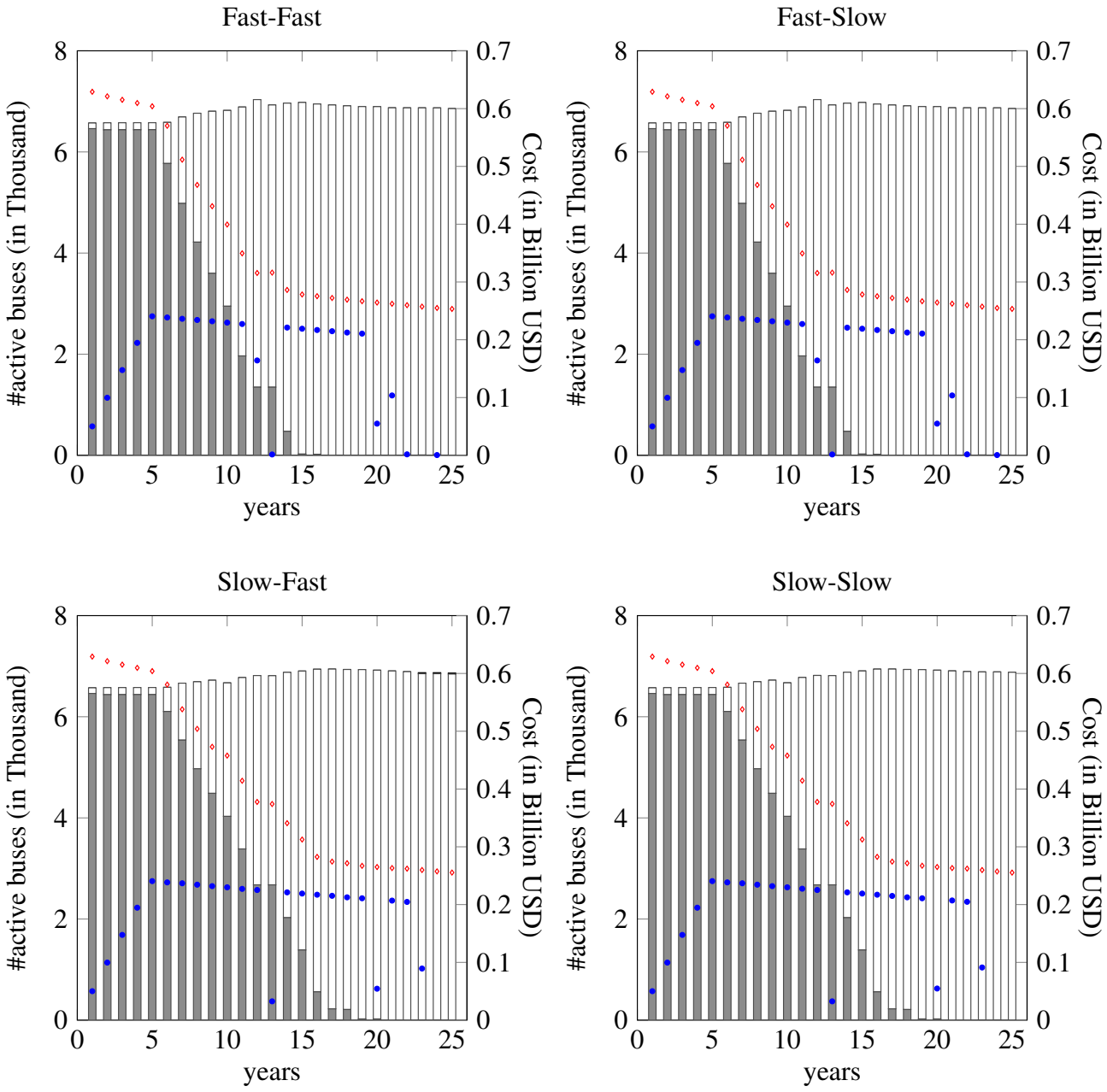

Figure D.19: Extended Scenario Tree - 3 By 2

Appendix D.3. Extended Scenario Tree - 2 By 3

We present the results of the Extended Scenario Tree - 2 By 3 case in Figure D.20. In this case, two branches for BEB technological improvements and three branches for HFCB technological improvements are considered in each stage. We used simplified assignment decisions, similar to the simplified base case

(Section Appendix D.1).

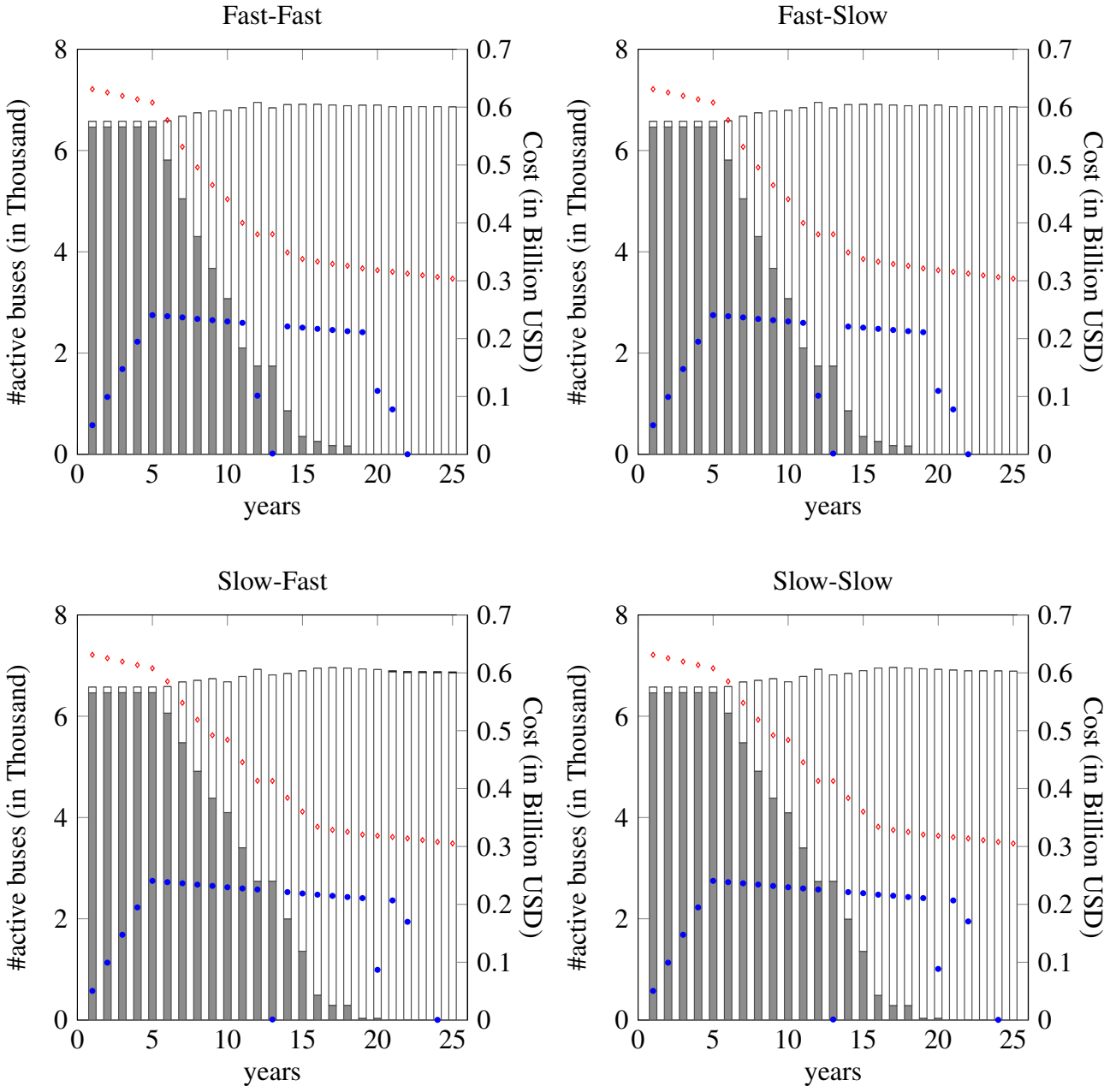

Figure D.20: Extended Scenario Tree - 2 By 3

CPU time is 26,039 seconds and the total expected cost is 14,111,360,587 USD, which increases to 14,137,237,734 USD after rounding the variables.